ELSEVIER

Agricultural and Forest Meteorology 113 (2002) 121–144

AGRICULTURAL AND FOREST METEOROLOGY

www.elsevier.com/locate/agrformet

# Eddy covariance flux corrections and uncertainties in long-term studies of carbon and energy exchanges

W.J. Massman [a,*], X. Lee [b]

[a] *USDA/Forest Service, Rocky Mountain Research Station, 240 West Prospect, Fort Collins, CO 80526, USA*
[b] *School of Forestry and Environmental Studies, Yale University, New Haven, CT 06511, USA*

Accepted 3 April 2002

**Abstract**

This study derives from and extends the discussions of a US DOE sponsored workshop held on 30 and 31 May, 2000 in Boulder, CO concerning issues and uncertainties related to long-term eddy covariance measurements of carbon and energy exchanges. The workshop was organized in response to concerns raised at the 1999 annual AmeriFlux meeting about the lack of uniformity among sites when making spectral corrections to eddy covariance flux estimates and when correcting the eddy covariance $CO_2$ fluxes for lack of energy balance closure. Ultimately, this lack of uniformity makes cross-site comparisons and global synthesis difficult and uncertain. The workshop had two primary goals: first, to highlight issues involved in the accuracy of long-term eddy covariance flux records; and second, to identify research areas and actions of high priority for addressing these issues. Topics covered at the workshop include different methods for making spectral corrections, the influence of 3D effects such as drainage and advection, underestimation of eddy covariance fluxes due to inability to measure low frequency contributions, coordinate systems, and nighttime flux measurements. In addition, this study also covers some new and potentially important issues, not raised at the workshop, involving density terms to trace gas eddy covariance fluxes (Webb et al., 1980). Wherever possible, this paper synthesizes these discussions and make recommendations concerning methodologies and research priorities.
Published by Elsevier Science B.V.

*Keywords:* Eddy covariance; Long-term flux records; Carbon balance

## 1. Introduction

The main scientific goals of the AmeriFlux network are to: (1) understand the factors and processes regulating $CO_2$ exchange, including soil processes, vegetation structure, physiology, and stage succession, and (2) determine principal feedbacks that may affect the future of the biosphere, such as responses to changes in climate, air pollution, and $CO_2$ concentrations (Wofsy and Hollinger, 1998). Because the eddy covariance method directly measures the net flux of $CO_2$, it is the logical choice for attempting measurements of the net $CO_2$ exchange to and from terrestrial ecosystems. However, implementing the eddy covariance method can vary significantly between sites. This is particularly true for $CO_2$ flux measurements which can be measured by either open- or closed-path systems (e.g., Leuning and King, 1992; Suyker nad Verma, 1993). Although the greatest difference in eddy

* Corresponding author. Fax: +1-970-498-1314.
*E-mail address:* wmassman@fs.fed.us (W.J. Massman).

0168-1923/02/$ – see front matter. Published by Elsevier Science B.V.
PII: S0168-1923(02)00105-3

covariance instrumentation is likely to be between open- and closed-path systems, there are also differences between sonic anemometer designs, sampling frequencies, processing algorithms, the relative geometries of the instruments, and the degree of aerodynamic interference by the measurement platform. To further complicate the issue of cross-site, long-term comparisons of net $CO_2$ exchange is the nearly uniform inability to close the surface energy balance. At most, if not nearly all, sites the energy available to drive evaporation, sensible heat, photosynthesis, and canopy storage almost always exceeds sum of these other processes by 10–20%. Because sensible and latent heat fluxes are measured by eddy covariance, the concern naturally arises about whether the net $CO_2$ flux is also underestimated and how or if to correct for this. Without some understanding of and ability to compensate for these differences, cross-site comparisons and global scale synthesis are difficult and uncertain at best. In an effort to address these site-to-site differences in flux systems and data processing, the National Institute for Global Environmental Change (NIGEC) sponsored an AmeriFlux workshop on 30 and 31 May, 2000 in Boulder, CO to address eddy covariance flux corrections and uncertainties in long-term studies of carbon and energy exchanges. The purpose of this paper is to synthesize, and where necessary extend, the discussions and conclusions of the workshop. Wherever possible, this paper also provides recommendations on methodologies and priorities for future research.

The remainder of this paper is divided into five sections. The next section discusses the fundamental equations of eddy covariance. Section 3 discusses the flux loss due to physical limitations of instrumentation, such as line averaging effects, sensor separation, data processing, and related issues that cause spectral attenuation of the flux. 2D and 3D effects, such as drainage and advection, are examined in Section 4. Section 5 discusses coordinate systems and Section 6 focuses specifically on night time flux issues. The paper closes with two appendices. Appendix A lists the workshop participants, speakers, and organizing committee. Appendix B provides a detailed discussion and derivation of the fundamental equations of eddy covariance. These equations are developed in three dimensions and include the WPL terms associated with fluxes of temperature and water vapor (Webb et al., 1980).

## 2. Fundamental equations of eddy covariance

### 2.1. Summary

In this section, we present the fundamental equations of eddy covariance. However, because we wish to be as general as possible, all fluxes are expressed as 3D vectors and the gradient operator, $\nabla$, should be understood as independent of coordinate system. Wherever necessary and appropriate, a coordinate system will be specified. The five fundamental equations, derived in Appendix B, detail the relationships between the various fluxes. Each equation is derived in a fully consistent manner with the minimum number of assumptions and wherever appropriate include heat and moisture effects. Here we present the results primarily as a summary and as background for later discussions.

Eq. (1) shows the relationship between the turbulent 3D temperature flux, $\overline{\mathbf{v}'T'_a}$, and the measured 3D sonic virtual temperature flux, $\overline{\mathbf{v}'T'_s}$, the measured turbulent 3D pressure flux, $\overline{\mathbf{v}'p'_a}$, and the 3D vapor covariance, $\overline{\mathbf{v}'\rho'_v}$. [Note here throughout this paper, we use the term covariance to mean that part of the turbulent flux exclusive of the WPL term (Webb et al., 1989 and Appendix B). The complete fluxes (or those turbulent fluxes that include the WPL term) are denoted with a superscript F, e.g., $\overline{\mathbf{v}'\rho'_v}^{F}$.]

$$\frac{\overline{\mathbf{v}'T'_a}}{\bar{T}_a} = \left[\frac{1}{1+\delta_{oc}\bar{\lambda}_v}\right]\frac{\overline{\mathbf{v}'T'_s}}{\bar{T}_s} - \left[\frac{\bar{\alpha}_v(1+\bar{\chi}_v)}{1+\delta_{oc}\bar{\lambda}_v}\right]\frac{\overline{\mathbf{v}'\rho'_v}}{\bar{\rho}_d} + \left[\frac{\bar{\beta}_v(2+\bar{\chi}_v)}{1+\delta_{oc}\bar{\lambda}_v}\right]\frac{\overline{\mathbf{v}'p'_a}}{\bar{p}_a} \quad (1)$$

where $\mathbf{v}'$ is the 3D turbulent (fluctuating) velocity; $\bar{\alpha}_v = 0.32\mu_v/(1+1.32\bar{\chi}_v)$; $\bar{\beta}_v = 0.32\bar{\chi}_v/(1+1.32\bar{\chi}_v)$; $\bar{\lambda}_v = \bar{\beta}_v(1+\bar{\chi}_v)$; $\bar{\chi}_v$ the volume mixing ratio or mole fraction for water vapor ($=\bar{p}_v/\bar{p}_d$); $\bar{p}_v$ the mean vapor pressure; $\bar{p}_d$ the mean partial pressure of dry air (i.e., ambient air devoid of water vapor); $\bar{p}_a$ the mean ambient pressure ($=\bar{p}_d+\bar{p}_v$); $\mu_v$ ($=m_d/m_v$) is the ratio the molecular mass of dry air, $m_d$, to the molecular mass of water vapor, $m_v$; $\bar{\rho}_d$ the mean ambient dry air density; $\bar{T}_s$ the mean temperature measured by sonic thermometry; $\bar{T}_a$ the mean ambient temperature and $\delta_{oc}=1$ for an open-path sensor and $\delta_{oc}=0$ for a closed-path sensor. We use the $\delta_{oc}$ notation to unify the mathematical development for

both the open- and closed-path systems. Note here that Eq. (1) assumes that the cross-wind correction to $T_s$ (Kaimal and Gaynor, 1991) is included in the sonic signal processing software and as such it does not explicitly appear in Eq. (1) (see Appendix B).

Eqs. (2) and (3) are the turbulent water vapor and $CO_2$ fluxes including the WPL terms as developed in Appendix B and adapted from Paw U et al. (1989) and Webb et al. (1980):

$$\overline{\mathbf{v}'\rho_v'}^{F} = (1+\bar{\chi}_v)\overline{\mathbf{v}'\rho_v'} + \bar{\rho}_v(1+\bar{\chi}_v)\left[\delta_{oc}\frac{\overline{\mathbf{v}'T_a'}}{\bar{T}_a} - \frac{\overline{\mathbf{v}'p_a'}}{\bar{p}_a}\right] \quad (2)$$

$$\overline{\mathbf{v}'\rho_c'}^{F} = \overline{\mathbf{v}'\rho_c'} + \bar{\rho}_c(1+\bar{\chi}_v)\left[\delta_{oc}\frac{\overline{\mathbf{v}'T_a'}}{\bar{T}_a} - \frac{\overline{\mathbf{v}'p_a'}}{\bar{p}_a}\right] + \bar{\omega}_c\mu_v\overline{\mathbf{v}'\rho_v'} \quad (3)$$

where $\bar{\rho}_c$ is the mean ambient $CO_2$ density, $\bar{\omega}_c$ $(=\bar{\rho}_c/\bar{\rho}_d)$ the mean mass mixing ratio for $CO_2$ and $\bar{\rho}_v$ the mean ambient water vapor density. As discussed in Appendix B, these two equations are generalizations of the original Webb et al. (1980) formulations. The major quantitative difference between Eqs. (2) and (3) and the corresponding formulations in Webb et al. (1980) is the 3D formulation and the inclusion of the pressure flux term, $\overline{\mathbf{v}'p_a'}$.

The total 3D water vapor ($\mathbf{F}_v$) and $CO_2$ ($\mathbf{F}_c$) fluxes are presented by Eqs. (4) and (5). These equations differ from Eqs. (2) and (3) only by the inclusion of the mean flow terms, $\mathbf{V}\bar{\rho}_v$ and $\mathbf{V}\bar{\rho}_c$:

$$\mathbf{F}_v = \mathbf{V}\bar{\rho}_v + \overline{\mathbf{v}'\rho_v'}^{F} \quad (4)$$

$$\mathbf{F}_c = \mathbf{V}\bar{\rho}_c + \overline{\mathbf{v}'\rho_c'}^{F} \quad (5)$$

where $\mathbf{V}$ is the mean 3D velocity vector.

The general equation for $CO_2$ mass conservation for application to long-term ecosystem studies of the $CO_2$ budget is given as

$$\bar{\rho}_d\frac{\partial\bar{\omega}_c}{\partial t} + [\overline{\mathbf{v}'\rho_d'}\cdot\nabla\bar{\omega}_c - \mathbf{V}\bar{\omega}_c\cdot\nabla\bar{\rho}_d] + \nabla\cdot(\mathbf{V}\bar{\rho}_c + \overline{\mathbf{v}'\rho_c'} - \bar{\omega}_c\overline{\mathbf{v}'\rho_d'}) = \bar{S}_c \quad (6)$$

where $t$ is the time, $\bar{S}_c$ the mean source/sink term for $CO_2$, $-\bar{\omega}_c\overline{\mathbf{v}'\rho_d'}$ the WPL term for $CO_2$ and $\overline{\mathbf{v}'\rho_c'}^{F} = \overline{\mathbf{v}'\rho_c'} - \bar{\omega}_c\overline{\mathbf{v}'\rho_d'}$ (Webb et al., 1980; Paw U et al., 2000, Appendix B). [We note here that for Eq. (6), we have dropped a small correction term to $\bar{S}_c$ related to the stoichiometry of photosynthesis and respiration (Appendix B).] The turbulent dry air flux, $\overline{\mathbf{v}'\rho_d'}$ is given as

$$\overline{\mathbf{v}'\rho_d'} = -\bar{\rho}_d(1+\bar{\chi}_v)\left[\delta_{oc}\frac{\overline{\mathbf{v}'T_a'}}{\bar{T}_a} - \frac{\overline{\mathbf{v}'p_a'}}{\bar{p}_a}\right] - \mu_v\overline{\mathbf{v}'\rho_v'} \quad (7)$$

Although not all issues raised by these equations were discussed at the workshop, it is important for the purposes of the workshop and this paper to discuss some of the implications of these equations to the practice of eddy covariance.

### 2.2. Some implications

The equation of mass conservation, Eq. (6), is the basis for long-term studies of the $CO_2$ budget. The traditional method of obtaining (an approximate) $CO_2$ budget over a 24 h period, usually involves the vertical component of Eq. (6) integrated over the vertical depth extending from the soil surface to height of the flux measurement. The storage (integral of the time rate of change term) and flux terms (integral of the flux divergence term) are each measured and summed over 24 h (e.g., Moncrieff et al., 1996; Lee, 1998). However, to date none of the $CO_2$ budget studies have included the second term of the left-hand side of Eq. (6), $[\overline{\mathbf{v}'\rho_d'}\cdot\nabla\bar{\omega}_c - \mathbf{V}\bar{\omega}_c\cdot\nabla\bar{\rho}_d]$, here called the quasi-advective term. Because of the component involving the dry air flux, $\overline{\mathbf{v}'\rho_d'}\cdot\nabla\bar{\omega}_c$, in the quasi-advective term, Eqs. (6) and (7) suggest that the vertical profiles of the water vapor, temperature, and pressure fluxes may also need to be measured. The potential importance of the dry air gradient term, $\mathbf{V}\bar{\omega}_c\cdot\nabla\bar{\rho}_d$, is less clear. Under most conditions, this term should be negligibly small. We expect this because dry air is likely to be well mixed so that horizontal components of $\nabla\bar{\rho}_d$ are probably insignificant in most situations. Over the depth of the profile measurements hydrostatic conditions do not appear to contribute significantly to $\nabla\bar{\rho}_d$ and mean velocities, $\mathbf{V}$, are generally quite low within a canopy.

Concerning the attenuation of temperature fluctuations for closed-path systems, we have found only one study that measures the attenuation of temperature fluctuations within a cylindrical tube. Frost

(1981) found that turbulent temperature fluctuations were reduced to the level of instrument noise beyond a downstream distance greater that about 11 tube diameters. This observation should be useful in ensuring the validity of $T'_a \rightarrow 0$ for current and future closed-path eddy covariance systems.

Throughout this study, we have included the pressure flux term, $\overline{\mathbf{v}p'_a}$, because there are special circumstances under which it may be important. Fig. 1 is a time course of the vertical pressure flux, $\overline{w'p'_a}$, for 2 days in January 2000. Also included on this figure is the ratio of $-\overline{w'p'_a}$ to $\bar{\rho}_a u_*^3$, where $u_*$ is the friction velocity. These are half hourly eddy covariance data obtained at a high elevation (3200 m) alpine site in southern Wyoming USA at a height of 27.1 m above the ground over a forest of approximately 18 m in height. Mean wind speeds during this period were between 5 and 15 m s$^{-1}$ and exceeded 10 m s$^{-1}$ for several hours at a time and $u_*$ exceeded 1 m s$^{-1}$ at all times. During this period $|(\overline{w'p'_a}/\bar{p}_a)/(\overline{w'T'_a}/\bar{T}_a)| \geq 20\%$. In other words, during periods of high winds and significant turbulence the pressure flux can contribute to the WPL term, $-\bar{\omega}_c\overline{\mathbf{v}'\rho'_d}$, for $CO_2$ or any other trace gas. Therefore, for an open-path system the pressure flux can be relatively significant. But, the implications to a closed-path systems are less obvious because there have been no studies (we are aware of) addressing the behavior of pressure fluctuations in turbulent tube flow. However, because $\overline{w'p'_a} \leq 0$, the possibility exists that any long-term $CO_2$ studies may have a bias in NEE resulting from ignoring this term during turbulent high wind speed conditions. For example, assuming that $\overline{w'p'_a} \approx -10$ Pa m s$^{-1}$ (Fig. 1), $\bar{p}_a \approx 10^5$ Pa, and $\bar{\rho}_c \approx 675$ mg m$^{-3}$, then the vertical pressure flux term, $-\bar{\rho}_c\overline{w'p'_a}/\bar{p}_a$, of Eq. (3) is approximately $+0.06$ mg $CO_2$ m$^{-2}$ s$^{-1}$ which can be a significant fraction of either the daytime or nighttime $CO_2$ flux. Over the course of a year this term would yield an additional 5.1 t C ha$^{-1}$ to the annual carbon balance of a (perpetually turbulent and windy) site. But, because the magnitude of $|\overline{w'p'_a}|$ is usually less than 10 Pa m s$^{-1}$, this additional 5.1 t C ha$^{-1}$ is likely to be the maximum possible amount.

In closing, the purpose of this section (and Appendix B as well) is to provide a framework that unifies the elements and discussions of the workshop. Although the workshop did not specifically focus on these fundamental equations, their presentation here allows each subject covered at the workshop to be referenced to a process or an equation, thereby allowing them to be more precisely defined and quantified. The next section discusses the spectral corrections associated with each of the covariance terms (given on the right-hand side) of Eqs. (1)–(7).

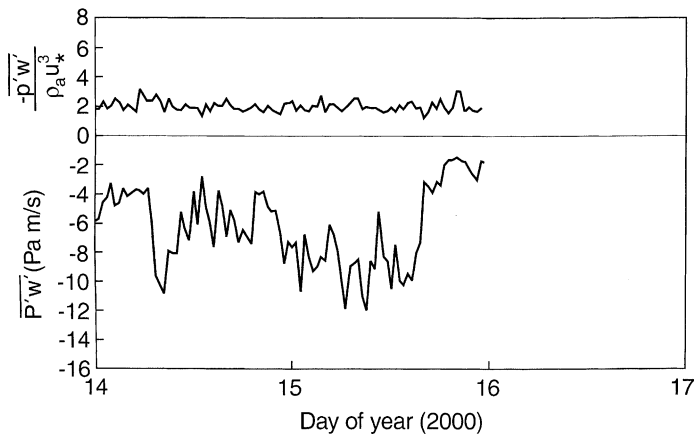


Fig. 1. Time course of half hourly eddy covariance data. The bottom curve is the vertical pressure flux, $\overline{w'p'_a}$ (Pa m s$^{-1}$), the top curve is the non-dimensionalized pressure flux, $-\overline{w'p'_a}/\bar{\rho}_a u_*^3$ (where $u_*$ is the friction velocity), and the zero line if highlighted. Data taken at a high elevation site in southern Wyoming USA between 14 and 16 January, 2000 under neutral, windy, and very turbulent atmospheric conditions ($u_* \geq 1$ m s$^{-1}$). Fluxes include spectral corrections using spectra developed from data obtained at the site. The non-dimensionalized flux indicates that $-\overline{w'p'_a}/\rho_a u_*^3 \approx 2$ for $z/L \approx 0$ in agreement with the observations of Wilczak et al. (1999).

## 3. Flux loss due to physical limitations of instrumentation

All eddy covariance systems attenuate the true turbulent signals at sufficiently high and low frequencies (e.g., Moore, 1986). This loss of information results from limitations imposed by the physical size of the instruments, their separation distances, their inherent time response, and any signal processing associated with detrending or mean removal (Moore, 1986; Horst, 1997; Massman, 2000, 2001; Rannik, 2001). There are a variety of ways to assess and correct the raw covariances for this loss of information. However, the workshop focused primarily on two methods. One method, proposed by Goulden et al. (1997), is termed the low-pass filtering method, and the other, proposed by Massman (2000, 2001), is termed the analytical approach. While neither is perfect or the ultimate solution to the problem of flux loss, comparison of the two methods showed the strengths and weaknesses of both. But, before discussing these two methods and detailing the differences between them, we must first define the concept of a transfer function, a first-order filter, and a low-pass recursive filter.

### 3.1. Preliminaries

The basic premise for describing the physical characteristics and behavior of a sensor or measuring instrument is that its dynamic performance can be modeled by an appropriate differential equation. The behavior of an ideal first-order instrument (or system) is defined by the following linear first-order non-homogeneous ordinary differential equation:

$$\tau_1 \frac{\mathrm{d}X_\mathrm{O}}{\mathrm{d}t} + X_\mathrm{O} = X_\mathrm{I}(t) \tag{8}$$

where $X_\mathrm{I}$ is the input or forcing function, $X_\mathrm{O}$ the output or response function, $t$ the time and $\tau_1$ the instrument's time constant. Eq. (8) can be used to assess the system's response to any type of forcing, but the response to sinusoidal forcing is of greatest interest because it is the basis for describing the response to much more complicated forcing. The steady-state solution to Eq. (8) assuming sinusoidal input, $X_\mathrm{I}(t) = A_\mathrm{I}\exp(-\mathrm{j}\omega t)$, is

$$X_\mathrm{O}(t) = \frac{A_\mathrm{I}\,\mathrm{e}^{-\mathrm{j}\omega t}}{1-\mathrm{j}\omega\tau_1} = \frac{X_\mathrm{I}(t)}{1-\mathrm{j}\omega\tau_1} \tag{9}$$

where $\mathrm{j} = \sqrt{-1}$, $\omega = 2\pi f$, $f$ the input forcing frequency (Hz) and $A_\mathrm{I}$ the amplitude of the input forcing. Note that throughout this study, we use complex notation because it simplifies the analysis.

The transfer function of a linear first-order sensor (system), $h_1(\omega)$, is the ratio of the output signal to the input signal, $X_\mathrm{O}(t)/X_\mathrm{I}(t)$, or

$$h_1(\omega) = \frac{1}{1-\mathrm{j}\omega\tau_1} = \frac{1+\mathrm{j}\omega\tau_1}{1+\omega^2\tau_1^2} = \frac{\mathrm{e}^{\mathrm{j}\phi_1(\omega)}}{\sqrt{1+\omega^2\tau_1^2}} \tag{10}$$

where $\phi_1(\omega)$ is the phase of the filter and is defined as $\tan^{-1}(\mathrm{Im}[h_1(\omega)]/\mathrm{Real}[h_1(\omega)])$.

Although not specifically derived by Horst (1997) or Massman (2000), Eq. (10) is the same function they use in their analyses. The major advantage of this general methodology of describing dynamic characteristics of sensors is that it allows the use of Fourier analysis to describe complex input and output signals in terms of an amplitude and phase characteristics. Because the system is linear the superposition principle applies and the input and output signals can be decomposed into their individual spectral components. Another advantage of this general approach is that it has a direct analog in electrical circuit design. For example, Eq. (10) is the same equation that describes an RL-circuit (e.g., Eugster and Senn, 1995) or an RC-circuit (or RC-filter). In the case of an RC-filter the time constant, $\tau_1$, is specifically identified as $RC$, the product of the circuit's resistance, $R$, and capacitance, $C$. Consequently the terminology used in circuit analysis and filtering can be applied to sensor input and response.

The first-order transfer function, Eq. (10), shows that for low frequencies (i.e., $\omega \to 0$) that $h_1(\omega) \to 1$ and that for high frequencies ($\omega \to \infty$) that $h_1(\omega) \to 0$. Therefore, the filter defined by Eq. (10) passes the low frequencies relatively unaffected and attenuates the high frequencies, thereby, defining a low-pass filter. The corresponding first-order high-pass filter, $h_1^{\mathrm{HP}}(\omega)$, is the complement of $h_1(\omega)$, i.e., $h_1^{\mathrm{HP}}(\omega) = 1 - h_1(\omega)$.

To this point, we have assumed that the input and output signals are continuous functions. In addition, we can also define the low-pass recursive filter in terms of a discretely sampled time series, noting that for any given filter applicable for continuous input and output, there is always an analog for discretely sampled input

and output. Consider a discrete equally spaced time series, $x_i$, where $i = 1, 2, 3, \ldots$ indicates the time $t_i$ at which the data are sampled. The difference equation for a first-order low-pass recursive filter is defined as follows:

$$y_i = Ay_{i-1} + (1 - A)x_i \tag{11}$$

where $x_i$ is the $i$th input datum, $y_i$ the $i$th output datum, $A = \exp(-1/(f_s\tau_r))$ with $f_s$ as the sampling frequency and $\tau_r$ as the filter time constant. Eq. (11) is the basis for the low-pass filtering procedure employed in some present eddy covariance systems. However, it is possible to develop filtering procedures using higher order recursive filters, i.e., ones with more recursive terms $(y_{i-2}, y_{i-3}, \ldots)$ or non-recursive filters, i.e., ones with more input terms $(\ldots, x_{i-2}, x_{i-1}, x_{i+1}, x_{i+2}, \ldots)$. But these more complicated filters are beyond the intent of the present study.

Eq. (11) is the low-pass complement of the high-pass recursive filter discussed in McMillen (1988), Moore (1986), Massman (2000, 2001), except that the time constant used in the present study does not have the same value as that used in Massman (2000, 2001). Its transfer function is the complement of Eq. (4) in Massman (2000) and is given as

$$h_r(\omega) = \frac{[1 - A][1 - A\ \cos(\omega/f_s) - jA\ \sin(\omega/f_s)]}{1 - 2A\ \cos(\omega/f_s) + A^2} \tag{12}$$

Although Eqs. (10) and (12) may appear different their moduli are functionally similar. This is the basis of Massman's (2000, Table 1) claims that the equivalent first-order time constant for $h_r(\omega)$ is equal to $\tau_r$ and for many references to Eq. (11) as an RC-filter as well. However, there is a relatively significant difference between the phases of these two filters. Fig. 2 compares the phases of a first-order filter and a recursive filter. The consequence of this phase difference will be discussed in the following section. Also, see Shaw et al. (1998) for an example of a first-order filter phase analysis, Berger et al. (2001) for an example of a phase analysis of the recursive filter, and Massman (2000) for an example of the potential importance of phases and phase shifts for flux attenuation.

### 3.2. Strengths and weaknesses of the two methods

When applying either of the two spectral correction methods some basis for estimating the specific corrections must first be defined. In the case of the low-pass filtering method, which is applied to closed-path systems, the sonic temperature flux and the universality of scalar spectra are the bases. For the analytical approach, the basis is defined by how well an instrument's transfer function can be approximated by a first-order filter and by how well the true cospectra, $Co_{w\beta}(f)$, for any given flux measurement, $\overline{w'\beta'}$, can be approximated by the following simple model of a

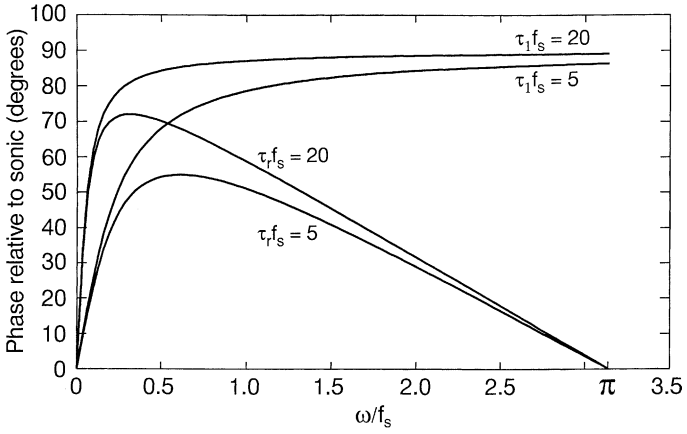


Fig. 2. Comparison of phase shifts associated with a first-order filter, Eq. (10), and a low-pass recursive filter, Eq. (12). Two cases are presented: one assuming that $\tau_1 f_s = \tau_r f_s = 5$ and the other $\tau_1 f_s = \tau_r f_s = 20$, where $\tau_1$ is the time constant for the first-order filter, $\tau_r$ the time constant of the recursive filter, and $f_s$ the sampling frequency. The method of calibrating the recursive filter results in $\tau_r = \tau_1$. Phase differences beyond the Nyquist frequency ($\omega/f_s = \pi$) are not included.

frequency-weighted normalized cospectrum:

$$\frac{f\mathrm{Co}_{w\beta}(f)}{\overline{w'\beta'}} = \frac{2}{\pi}\frac{f/f_x}{1+(f/f_x)^2} \tag{13}$$

where $f_x$ is the frequency at which $f\mathrm{Co}_{w\beta}(f)$ reaches its maximum, or, in the case of the model cospectrum given by Eq. (13), $f_x$ is also the 'mid-point' of the cospectral power, i.e., the cospectral power contained in the frequency bands $[0, f_x]$ and $[f_x, \infty]$ are both equal to 50% of the total cospectral power. One obvious approximation that results from Eq. (13) is that the high frequency cospectral power decays as $f^{-2}$, unlike true cospectra which typically decay as $f^{-7/3}$. The consequences of this and other approximations associated with the analytical method can vary with wind speed and atmospheric stability, but tend to be small during unstable atmospheric conditions for eddy covariance systems that have a little instrument related filtering (Massman 2000, 2001).

To use the analytical approach, $f_x$ must be provided externally or developed by generalizing results from observed cospectra. For example, Moore (1986), Horst (1997), and Massman (2000) all used models adapted from Kaimal et al. (1972) to parameterize $f_x$ as a function of stability; whereas, Wyngaard and Coté (1972) developed models of $f_x$ using inertial subrange arguments. Nevertheless, the analytical approach is not necessarily limited to previous models of $f_x$. More precise site-specific models of $f_x$ could also be used with the analytical approach.

A significant advantage that the low-pass filtering method has over the analytical method is that the accuracy of the former is not dependent upon any specific cospectral shape, whereas for the analytical method it is (Massman, 2000). This distinction is likely to be most important for situations or sites with highly variable cospectra. However, to date no quantitative comparison of the two methods has actually been performed and we recommend that such a comparison be conducted. Other important differences and further strengths and weaknesses are detailed in the following discussions.

To implement the low-pass filter method requires determining the effective first-order time constant for the filter. This can be accomplished by several methods. One method is to supply a step change in $CO_2$ concentration at the mouth of the intake tube (e.g., from zero to ambient concentration or vice versa) and then estimate the time constant associated with the time decay or rise of the signal (Munger et al., 1996). This time constant is the effective first-order time constant, $\tau_1$. Another method is implemented as follows. First, spectra of the sonic temperature and $CO_2$ (or any other trace gas) are calculated and compared. Next, the low-pass filter, Eq. (11), is applied to the sonic temperature data stream and the time constant $\tau_r$, is adjusted until the filtered temperature spectra resemble the $CO_2$ spectra (see Hollinger et al., 1999). A third method uses the frequency dependent phase characteristics of the $CO_2$ signal relative to, e.g., the sonic temperature signal to infer both the time lag between the sonic and the intake tube and the first-order time constant, $\tau_1$, of the $CO_2$ system (e.g., Lenschow et al., 1982; Shaw et al., 1998). Fundamentally, all procedures accomplish the same thing—they calibrate the recursive filter so that the filter time constant accounts for the effects of the signal attenuation associated with tube flow and the analyzer, i.e., $\tau_r = \tau_1$ and all methods should produce approximately the same value for the effective time constant. But, regardless of the method for estimating $\tau_1$ or $\tau_r$ the same algorithm is employed for correcting the $CO_2$ flux.

To examine this algorithm mathematically, let $h_T(\omega)Z_T$ be the Fourier transform of the measured temperature time series and $h_c(\omega)Z_c$ be the Fourier transform of the measured $CO_2$ signal. Here the Fourier transform of the true (unfiltered) atmospheric fluctuations in temperature is $Z_T$ and for $CO_2$ it is $Z_c$. The transfer function $h_T(\omega)$ includes the filtering effects associated with sonic line averaging (see Moore, 1986 or Massman, 2000 and references therein) or with the intrinsic properties of any separate fast response temperature sensor. The transfer function $h_c(\omega)$ is associated with tube flow and the trace gas analyzer attenuation. The Fourier transform of the recursively filtered temperature time series is $h_r(\omega)h_T(\omega)Z_T$. Calibrating the recursive filter matches the spectrum of the filtered temperature signal with the spectrum of $CO_2$, which yields the following approximation:

$$[h_r(\omega)h_T(\omega)Z_T][h_r(\omega)h_T(\omega)Z_T]^* \approx [h_c(\omega)Z_c][h_c(\omega)Z_c]^* \tag{14}$$

where $^*$ denotes complex conjugation. Next assuming similarity between the true (unfiltered) temperature

spectrum, $Z_T Z_T^*$, and the true scalar spectrum, $Z_c Z_c^*$, yields

$$|h_r(\omega)^2||h_T(\omega)|^2 \approx |h_c(\omega)|^2 \tag{15}$$

where $|h(\omega)|^2 = h(\omega)h^*(\omega)$. The filtering effect associated with sonic line averaging can be expected to be much smaller than that associated with the recursive filter provided that the height of the sensors above the surface greatly exceeds the sonic path length. As this is typically the case, it follows immediately that for a properly tuned recursive filter, $|h_r(\omega)^2| \approx |h_c(\omega)|^2$. Therefore, tuning the recursive low-pass filter matches the modulus of the filters. Next we investigate the consequences of applying the calibrated low-pass filter technique to the cospectrum (fluxes). For this, we apply the same Fourier analysis used in Eqs. (14) and (15) to the flux case.

The simplest flux correction factor based on the low-pass filter technique is the ratio of the measured sonic temperature flux, $\overline{w'T'_s}$, to the temperature flux calculated with the filtered temperature, $\overline{w'T'_{sr}}$. [Note that before filtering $T'_s$, it is shifted by the corresponding $CO_2$ lag time.] Therefore, the $CO_2$ covariance corrected for high frequency flux loss is $[\overline{w'T'_s}/\overline{w'T'_{sr}}]\overline{w'\rho'_c}$. Using the Fourier transform method on $[\overline{w'T'_s}/\overline{w'T'_{sr}}]\overline{w'\rho'_c}$ yields the following expression for the corrected complex cospectrum, $C^C_{wc}$:

$$C^C_{wc} = \frac{[h_w(\omega)Z_w][h_T(\omega)Z_T]^*}{[h_w(\omega)Z_w][h_r(\omega)h_T(\omega)Z_T]^*} \times [h_w(\omega)Z_w][h_c(\omega)Z_c]^* \, e^{-j\phi_{wc}(\omega)} \tag{16a}$$

where the denominator, $[h_w(\omega)Z_w][h_r(\omega)h_T(\omega)Z_T]^*$, is the transform of the recursively filtered covariance $\overline{w'T'_{sr}}$; the numerator, $[h_w(\omega)Z_w][h_T(\omega)Z_T]^*$, the transform of the covariance $\overline{w'T'_s}$; $[h_w(\omega)Z_w][h_c(\omega)Z_c]^*$ the transform of the covariance $\overline{w'\rho'_c}$; $h_w(\omega)$ the filter associated with line averaging of the sonic vertical velocity signal $w'$ and $\phi_{wc}(\omega)$ has been introduced to account for the possibility of a shift in phase (or time) between the sonic and $CO_2$ signals caused by any longitudinal separation between the sonic sensing path and the closed-path intake tube or any unresolved lag time after performing digital time shifts to resynchronize the sonic and closed-path sensor time series (e.g., Massman, 2000). Simplifying the right-hand side of this equation yields

$$C^C_{wc} = \frac{h_w(\omega)h_c^*(\omega)}{h_r^*(\omega)} \, e^{-j\phi_{wc}(\omega)}[Co - jQa] \tag{16b}$$

where the complex cross spectrum, $Z_w Z_c^*$, has been replaced by $[Co - jQa]$ with Co as the true cospectrum and Qa as the quadrature spectrum (Kaimal and Finnigan, 1994). Finally recognizing (a) that $h_w(\omega)$ is real, i.e., sonic line averaging does not cause a phase shift or time delay between $w'$ and $\rho'_c$ (Kristensen and Fitzjarrald, 1984) and (b) that the real part of $C^C_{wc}$, denoted $Co^M_{wc}$, is the measured cospectrum after correction by the recursive filter yields

$$Co^M_{wc} = h_w(\omega)\text{Real}\left\{\left[\frac{h_c^*(\omega)\, e^{-j\phi_{wc}(\omega)}}{h_r^*(\omega)}\right][Co - jQa]\right\} \tag{16c}$$

An examination of the right-hand side of Eq. (16c) clarifies some of the compromises associated with the low-pass filter method. First, it does not correct for sonic path or line averaging effects $[h_w(\omega)]$ or for possible phase (time) shifts inherent in the relative placement of the sensors or residual lag times $[\exp(-j\phi_{wc}(\omega))]$. Second, the phase difference between $h_c(\omega)$ and $h_r(\omega)$ is not accounted for in this approach. This second issue can be significant in some situations. For example, Fig. 2 shows the difference between the phases of a first-order system, which $h_c(\omega)$ is assumed to be, and the recursive filter, $h_r(\omega)$. For relatively low frequencies, $\omega/f_s < 0.1$, the phase difference is small, but it does increase rapidly as $\omega$ increases. Therefore, for scenarios where most of the cospectral power is well sampled and located in relatively low frequencies (e.g., $f_x/f_s < 0.01$), the phase difference is of little consequence because the associated effect (i.e., uncorrected flux loss) is confined to frequencies that carry very little cospectral power. But, for other cases where, e.g., $f_x/f_s \geq 0.1$ the measured (but low-pass corrected) flux could be significantly underestimated if the effects of the phase difference are not accounted for. [Note here we use a value of 0.1 as a cutoff for $\omega/f_s$ because it summarizes the results of Fig. 2 relatively well. But, as Fig. 2 also shows, the cutoff value is in fact more precisely determined by the values of $\tau_r f_s$ and $\tau_1 f_s$.]

An analysis similar to that provided by Eqs. (16a)–(16c) shows that attempting to eliminate the phase

difference between $h_c(\omega)$ and $h_r(\omega)$ by low-pass filtering $w'$ is not necessary. In this formulation of the low-pass filtering method, the corrected flux $\overline{w'\rho'_c}^C$ is estimated by $[\overline{w'T'_s}/\overline{w'_r T'_{sr}}]\overline{w'_r\rho'_c}$, where $w'_r$ is the recursively filtered sonic vertical velocity time series. This analysis results in an expression similar to Eqs. (16b) or (16c) and all the compromises associated with the low-pass filter method remain. The fundamental concern here with the low-pass filter method is that calibrating the recursive filter constrains only the magnitude (modulus) of the filter, Eq. (15), without constraining the phase difference between $h_c(\omega)$ and $h_r(\omega)$ or accounting for $h_w(\omega)$ or $\exp(-j\phi_{wc}(\omega))$.

In theory, the analytical method includes corrections for the phase differences (time shifts) between the various sensors (Massman, 2000). However, this method does assume that for a given period (of approximately one-half hour) of flux data the observed cospectra can be well approximated by a relatively smooth function (i.e., Eq. (13) above). Unfortunately, most observed (half hourly) cospectra show significant variability from one cospectral estimate to another. Consequently, they are not necessarily very smooth and the analytical approach may produce correction factors that can be in error (Massman, 2000; Laubach and McNaughton, 1999). The low-pass filter method does not suffer from this problem because it is applied directly to the eddy covariance time series (Eq. (11) above) rather than to the flux.

On the other hand, the analytical method includes corrections for low frequency losses due to any recursive high-pass filtering (McMillen, 1988), linear detrending of the eddy covariance time series (Gash and Culf, 1996), or mean removal (Kaimal et al., 1989; Kristensen, 1998; Massman, 2000), whereas the low-pass filter method does not. These low frequency losses may be of greater importance than has been attributed to them in the past because (a) the frequency-weighted spectra (and by implication the cospectra) of (Kaimal et al., 1972) actually result from too much high-pass filtering (Högström, 2000), (b) the surface layer may be disturbed during flux measurement periods (McNaughton and Laubach, 2000), or (c) significant flux-bearing low frequencies have been inadvertently removed from the data during processing (Finnigan et al., 2002). All three of these possibilities imply that true cospectral power may actually be distributed more uniformly across frequencies near $f_x$ than can be well approximated by Eq. (13). Nevertheless, Massman (2000, 2001) shows that the analytical method can be adapted to account for this possible broadening of true cospectra.

In addition to providing estimates of the eddy covariance correction factors, the analytical method is also useful for planning and design of eddy covariance systems. Following the notation of Massman (2000, 2001), the general criteria for minimizing errors due to the relative placement of sensors and time response characteristics is summarized by the following expressions:

$$2\pi f_x \tau_h \gg 1 \tag{17a}$$

$$2\pi f_x \tau_b \gg 1 \tag{17b}$$

$$2\pi f_x \tau_e \ll 1 \tag{17c}$$

where $\tau_h$ is the equivalent time constant associated with trend removal (McMillen, 1988; Gash and Culf, 1996), $\tau_b$ the equivalent time constant associated with block averaging and mean removal (Kaimal et al., 1989; Kristensen, 1998; Massman, 2001) and $\tau_e$ is the equivalent first-order time constant for the entire set of low-pass filters associated with sonic line averaging, sensor separation, finite response times, etc. [see Table 1 and Eq. (9) of Massman, 2000]. If these three criteria are met then the analytical method suggests little need for spectral correction.

Finally, the low-pass filter method is questionable during conditions when the magnitude of the heat flux is less than about $10\,W\,m^{-2}$. When this occurs $|\overline{w'T'_s}| \approx 0$ and $|\overline{w'T'_{sr}}| \approx 0$ and the low-pass filter correction term becomes undefined. Similarly, the analytical method is suspect for very stable atmospheric conditions because correction factors for $CO_2$ fluxes can exceed 1.5 or even 2.0 (Massman, 2001). Ultimately, neither correction method is likely to be useful for conditions where the turbulent transfer is dominated by intermittent events because all eddy covariance measurements become less reliable under such conditions.

## 4. Flux error due to 2D and 3D effects

A major goal of many micrometeorological studies is to quantify the net exchange of a trace gas of interest

between the atmosphere and the surface. This is usually achieved by approximating the net exchange with the measured vertical eddy flux corrected for storage below the level of measurement and thereby ignoring all the other terms of the mass conservation equation because they are difficult to measure. This approximation works if the flow and scalar fields are nearly horizontally homogeneous. However, under 2D and 3D influences the vertical eddy flux may systematically deviate from the true net exchange. Mathematically this is expressed by integrating Eq. (6) from the soil surface ($z = 0$) to some height ($z = z_m$) at which the flux measurements are made, yielding:

$$\int_0^{z_m} \bar{\rho}_d \frac{\partial \bar{\omega}_c}{\partial t}\,dz + \int_0^{z_m} [\overline{\mathbf{v}'\rho_d'} \cdot \nabla\bar{\omega}_c - \mathbf{V}\bar{\omega}_c \cdot \nabla\bar{\rho}_d]\,dz + \int_0^{z_m} \nabla_H \cdot \mathbf{V}\bar{\rho}_c\,dz + \int_0^{z_m} \nabla_H \cdot \overline{\mathbf{v}'\rho_c'}^F\,dz + W(z_m)\bar{\rho}_c(z_m) + \overline{w'\rho_c'}^F(z_m) = \int_0^{z_m} \bar{S}_c\,dz + W(0)\bar{\rho}_c(0) + \overline{w'\rho_c'}^F(0) \quad (18)$$

where the first term on the left is the storage term, the second is the integrated form of the quasi-advective term (and has never been previously included in the budget equation before), the third term is related to the mean horizontal advective term with $\nabla_H$ as the horizontal gradient operator, the fourth term is the vertically integrated horizontal flux divergence, and the fifth term on the left is the measured (mean plus turbulent) flux with $W$ as the mean vertical velocity and $w'$ as the fluctuating component of the vertical velocity. The term on the right side of Eq. (18) is the net ecosystem exchange. We include the mean velocity term, $W(0)\bar{\rho}_c(0)$, as part of the net ecosystem exchange primarily for mathematical completeness. In many situations, it is reasonable to assume that $W(0) = 0$. However, there may be scenarios, possibly related to pressure pumping, where $W(0)$ during a flux-averaging period, although small, may not be 0.

Simpler forms of Eq. (18) or Eq. (6) have been used in many previous studies of 2D and 3D effects. For example, local 2D advection in which there is a step change in the surface source strength of a passive scalar has been studied by Philip (1959) and further developed by Dyer (1963) to estimate the so-called fetch-height ratio and by Schmid (1994) for footprint analyses. 2D changes in scalar fluxes caused by step changes in surface roughness have also been studied (e.g., Mulhearn, 1977; Lee et al., 1999) and previously reviewed by Garratt (1990). Nevertheless, any guidelines developed from these previous studies, while helpful, cannot be used with assurance of eliminating either 2D and 3D effects or the concomitant possibility of biases in the measured fluxes. There are several reasons for this. First, no previous study has considered the full complexity of Eqs. (6) and (18). Second, almost all studies reviewed by Garratt (1990) have assumed near-neutral atmospheric stability, consequently their results may not be accurate under extreme conditions, such as very stable air or free convection. Third, mesoscale motions, which are not included in these studies and which can bias vertical flux measurements, occur on 2D and 3D scales much larger than the scale of micrometeorology measurements, which can be characterized by site fetch and height scales. Thermally driven circulations, such as a land-lake breeze and stationary convective cells, and drainage flows are examples of 3D motions that may subject observations to advective influences. Fourth, these earlier micrometeorological studies assume no variation in background topography.

Clearly, a proper understanding of 2D and 3D flows and their role in micrometeorological flux observation is of importance to any site, but the problem of 2D and 3D flows is most difficult to treat at sites on non-flat topography. At least four topographic effects are relevant to the surface layer flux observations:

(1) Terrain can generate its own nighttime gravitational or drainage flows. A good example of this is the Walker Branch forest (Baldocchi, 2000). This forest is situated on a ridge top and nighttime wind speed tends to be low (mean nighttime friction velocity 0.15 m s$^{-1}$; KB Wilson, personal communication). These two characteristics favor the occurrence of drainage flow. At other sites on more even terrain, drainage flow is more likely to be driven by background topography larger than the tower footprint/fetch scale. Models of drainage flow have been developed for simple topography without vegetation (e.g., Brost and Wyngaard, 1978). However, at present, we lack models for the air layer within the height of the tower.

(2) Terrain obstacles can modify the ambient flow via a bluff body effect. Because the streamline in the tower air layer can depart significantly from the local terrain surface, persistent mean vertical motion may be expected. The severity of vertical advection will depend on vertical concentration gradient of the scalar of interest. Change of turbulent stress in response to the change in wind field may produce spatial variation of the scalar flux and hence horizontal advection (Finnigan, 1999). An analytical solution for advective flow over isolated low hills under neutral stability was first proposed by Jackson and Hunt (1975). This theory was later extended to canopy flow on hills (Finnigan and Brunet, 1995; Wilson et al., 1998) and to scalar concentration fields (Raupach et al., 1992). However, the utility of solutions of the Jackson and Hunt type in elucidating the advection problem is subject to debate (Finnigan, 1999; Lee, 1999).

(3) Surface source strength may not be uniform in the streamwise direction. For example, Raupach et al. (1992) showed that significant horizontal (along slope) advection of energy can result from variations in the incident solar radiation along a curved slope.

(4) Gravity waves generated by terrain obstacles are beyond the scope of traditional micrometeorology because of the extent of their horizontal spatial scales and their 3D nature. This motion type is common in stratified air with moderately strong winds (Smith, 1979). Their role in the surface-air fluxes is yet to be understood.

## 5. Issues arising from choice of coordinate systems and data processing

To date, the most common coordinate system used for flux measurements is a rectangular coordinate system sometimes called the 'natural' coordinate system (Tanner and Thurtell, 1969; Kaimal and Finnigan, 1994) or the 'streamline' coordinate system (Wilczak et al., 2001). In this coordinate system, the $x$-axis is parallel to the local mean horizontal wind ($U$) and the $z$-axis is perpendicular to the $x$-axis, thus the mean cross-wind ($V$) and the mean vertical wind ($W$) are zero. A third rotation, which minimizes the cross-stream stress term $\overline{w'v'}$, is also part of the natural coordinate system. But, it can introduce additional noise or uncertainty into the flux estimates (Wilczak et al., 2001) and is often ignored in many flux studies. Furthermore, there may be dynamical and diagnostic reasons why $\overline{w'v'}$ should not be minimized (Weber, 1999; Wilczak et al., 2001).

The main application of the natural coordinate system is for the calculation of fluxes in sloping terrain and there are several valid reasons for working in this particular coordinate system in non-uniform terrain (Wilczak et al., 2001). However, a major disadvantage to long-term studies is the possibility that $W \neq 0$ during the flux-averaging periods. Setting $W = 0$ for every half an hour (a) eliminates the mean flow component of the flux, thereby causing either a significant bias or a systematic underestimation of the individual fluxes and in the long-term balance (Lee, 1998) and (b) filters (attenuates) the low frequency components of the turbulent flux (Finnigan et al., 2002). Wilczak et al. (2001) and Paw U et al. (2000) outline a method, termed planar fit method, that can be used to estimate $W$. In fact, the planar fit method defines the preferred coordinate system for single point (single tower) flux measurements (Finnigan and Clement, in preparation). However, unlike the natural coordinate system, the planar fit method cannot be used in real time for each flux-averaging period. Rather it must be used over a set of many flux-averaging periods. Nevertheless, the planar fit method has been shown to reduce sampling errors (or the variability from one flux-averaging period to another) for flux data sets obtained over water (Wilczak et al., 2001). This method has yet to be tested over land in complex terrain and we recommend that it be evaluated for its impact on long-term $CO_2$ fluxes and carbon balances.

In addition to the two coordinate systems just described, there is another coordinate system that can be used for estimating fluxes in complex terrain (Finnigan, 1983). For studies of the vertical flux divergence, $\partial\overline{w'c'}/\partial z$, this particular streamline coordinate system is recommended because it should give the most reliable estimate of the flux divergence in curved flows than with Cartesian coordinate systems.

A second data processing issue concerns the possible loss of the low frequency portion of measured fluxes. For example, choosing a flux-averaging period that is too short will attenuate the low frequencies components of the flux (Lenschow et al., 1994;

Mann and Lenschow, 1994; Kristensen, 1998), as will overfiltering with any high-pass (e.g., recursive) filter (Högström, 2000). Loss of these low frequency components has been implicated in the lack of energy balance closure (Sakai et al., 2001; Finnigan et al., 2002) and in a 10–40% underestimation of the daytime $CO_2$ fluxes over forests (Sakai et al., 2001). Coordinate rotation can also act as a complicated non-linear high-pass filter (Finnigan et al., 2002). One possible solution to this problem involves using the raw (fully sampled) high frequency data without filtering and evaluating the fluxes with the planar fit method. Potentially this approach could circumvent many of the concerns about low frequency losses. Nevertheless and subject to the constraints outlined in Section 3 above, the analytical method should be able to correct the fluxes regardless of whether the data are recursively high-pass filtered or not (Massman, 2001). However, cospectra that describe the appropriate flux energy distribution is still required for the analytical approach. Such cospectra need not be the same as the cospectra of Kaimal et al. (1972) (e.g., Sakai et al., 2001).

## 6. Nighttime flux measurements: a co-occurrence of all eddy covariance limitations

Almost all eddy covariance limitations occur at night when the air becomes stably stratified. Some of these are instrumental, others are meteorological. The instrumental limitations ultimately result from the fact that eddy covariance instruments are best suited for daytime convective conditions when the dominant turbulent motions are frequent and large enough that sensor limitations are not significant. At night or during stable atmospheric conditions, when turbulent motions shift toward relatively higher frequencies and become more intermittent, the lack of instrument response due to finite time constant, sensor separation, path-length averaging, and tube attenuation becomes a severe limitation. Corrections developed with either the analytical method or the low-pass filtering method are suspect under very stable conditions.

Some of the meteorological limitations include large footprints, gravity waves, advection, and aerodynamic or low turbulence issues.

*Large footprints*. It is known that the eddy covariance footprint expands rapidly as air becomes increasingly stratified (Leclerc and Thurtell, 1990; Schmid, 1994) and can extend beyond the vegetation type under investigation. Footprint correction is however not straightforward as the existing footprint models are built on principles of eddy diffusion established for conditions of near-neutral stability. For example, air stability over a forest often exceeds the range over which the empirical Monin–Obukhov similarity functions are valid.

*Gravity waves*. Shear-generated gravity waves are a common motion type in the canopy at night (Lee and Barr, 1998; Fitzjarrald and Moore, 1990; Paw U et al., 1989, 1990). The wave motion manifests itself in the form of periodic time series of velocities, temperature and scalar concentrations. Strictly speaking, the stationarity condition is not satisfied during gravity wave events because the coefficient of auto-correlation does not vanish at a finite lag time and consequently no integral time scale can be defined. Numerical simulations show that a constant flux layer does not exist in the presence of the wave motion (Hu et al., 2002). Instead, fluxes of momentum and scalars can very greatly with height over the canopy with the flux peaking at the so-called critical level, i.e., the height at which the wave propagation speed matches the mean wind speed. For these reasons, eddy fluxes appear very noisy during a gravity wave event. However, when averaged over a long enough time period $CO_2$ fluxes collected at the Borden forest during a gravity wave event show the same dependence on soil temperature established for other periods (Lee, unpublished data). This suggests that although the raw data may appear noisy, the wave motion does not introduce a detectable systematic bias into the ensemble averaged fluxes.

*Advection*. Under very stable conditions, the vertical gradient of the Reynolds stress is small within the vegetation and therefore the horizontal pressure gradient, associated with baroclinic forcing (Wyngaard and Kosovic, 1994), synoptic weather systems, or the gravitational force on a slope (Mahrt, 1982), is relatively large. Simultaneously, large vertical gradients in scalar quantities exist near the ground due to the lack of vigorous turbulent mixing. Under these conditions, air motions within the canopy and surface layer are inherently 2D or 3D and the resulting drainage or (vertical and horizontal) advection that occurs is

likely to be of a magnitude much larger than that occurring in the daytime (e.g., Sun et al., 1998; Mahrt et al., 2001). This diel asymmetry could introduce a large bias into the estimates of annual net ecosystem production (Lee, 1998).

*Aerodynamic issues*. A common phenomenon at long-term flux sites is that turbulent $CO_2$ flux approaches zero as the level of turbulence, measured by the friction velocity, drops to zero (Goulden et al., 1996). This should be expected on the basis of aerodynamic reasoning. For example, both K-theory and Monin–Obukhov similarity theory suggest that in general turbulent scalar fluxes are proportional to $u_*(\partial c/\partial z)$. In other words, as the turbulence decreases so also must the turbulent fluxes. Fig. 3 is an example of the observed dependence of nighttime vertical $CO_2$ flux, $\overline{w'\rho_c'}^F$, on friction velocity, $u_*$. However, several issues remain unsettled during conditions of low turbulence.

Wofsy et al. (1993) and Goulden et al. (1996) suggest that biological source strength of $CO_2$ is not a function of air movement, implying that the storage corrected eddy flux should be independent of $u_*$ if the 1D approach accurately approximates the surface layer mass balance. Numerous observations show however that storage correction does not bring the flux to the same level as observed at high wind conditions (Fig. 4). In some cases, one can identify a critical or threshold friction velocity, $u_{*c}$, beyond which the flux seems to level off, while in other cases no threshold exists (e.g., Fig. 3 and windy sites reported by Aubinet et al. (2000)). Similarly, energy balance closure is generally poor at low $u_*$ conditions and improves as $u_*$ increases (Black et al., 2000; Aubinet et al., 2000). A common practice is to replace the flux during periods with $u_* < u_{*c}$ by the flux estimated with a temperature ($Q_{10}$) function established using data obtained during well-mixed, windy periods ($u_* > u_{*c}$). (Here $Q_{10}$ is the relative increase in respiration resulting from a 10 °C increase in temperature.) Lavigne et al. (1997) use a single $u_{*c}$ across all sites in a comparative study of nighttime eddy flux and chamber flux of $CO_2$. However, it is now recognized that $u_{*c}$ and $Q_{10}$ are site-specific parameters (Table 1). Another concern with the $u_{*c}$–$Q_{10}$ approach is the risk of double counting due to morning flush of $CO_2$ (Grace et al., 1995; Aubinet et al., 2000). Studies of the sensitivity of annual NEP to $u_{*c}$ suggest that imposing a $u_*$ threshold will increase the annual estimate of NEP by 0.5 t C ha$^{-1}$ per year or more (Grelle, 1997; Aubinet et al., 2000; Goulden et al., 1996; Barr et al., 2002).

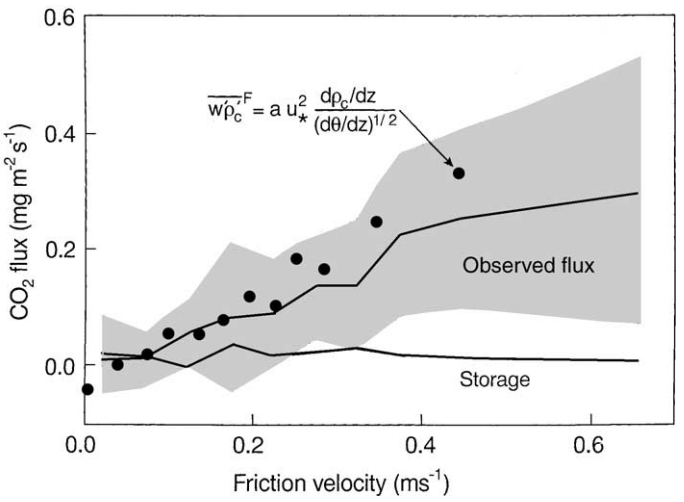


Fig. 3. Dependence of nighttime air storage and vertical eddy $CO_2$ flux, $\overline{w'\rho_c'}^F$, on friction velocity, $u_*$, at the Great Mountain Forest during May–September 1999. Data are averaged over 0.05 m s$^{-1}$ bins. Shaded area is one standard deviation about the mean flux. Dots are flux predictions based on Monin–Obukhov similarity theory for very stable air, where $a = -(0.25\theta/g)^{1/2}$, $\theta$ the potential temperature, $g$ the gravitational acceleration, and $\rho_c$ the $CO_2$ concentration. The F superscript indicates that the fluxes include the WPL terms.

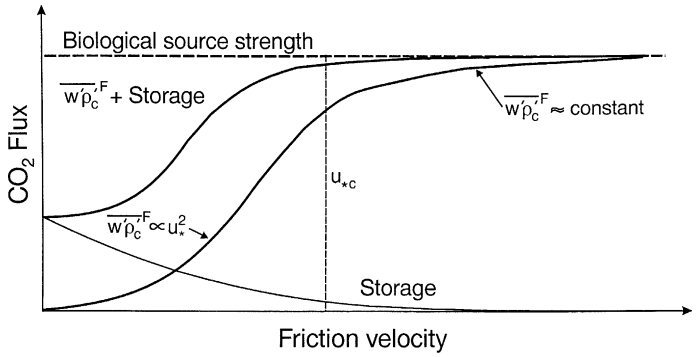


Fig. 4. Schematic diagram showing nighttime $CO_2$ eddy flux and air storage as a function of friction velocity. The F superscript indicates that the fluxes include the WPL terms.

The assumption that biological source strength is invariant with turbulence intensity is reasonable, except for the possibility of pressure pumping effects. Variations in barometric pressure at the ground surface are correlated with turbulence intensity (Shaw and Zhang, 1992). Such variations will introduce advective air movement into and out of the soil, thus enhancing the soil efflux of gases with concentrations exceeding ambient concentrations (Hillel, 1980). The pressure pumping effect has been proposed as the possible cause of episodic emissions of $CO_2$ from soils (Baldocchi and Meyers, 1991) and snowpacks (Yang, 1998, Y. Horazano, personal communication). Model simulations by Massman et al. (1997) suggest that the turbulent pressure pumping effect can increase or suppress the diffusive flux through a snowpack by 25% and the effect may be significantly more important for a variety of soils (Hillel, 1980; Nilson et al., 1991). Quasi-stationary pressure fields induced by wind blowing over rough topography could further enhance diffusional fluxes significantly more than ground level turbulent pressure fluctuations (Farrell et al., 1966; Colbeck, 1989). Although pressure fluctuations are not a standard parameter called for by the AmeriFlux science plan (Wofsy and Hollinger, 1998), further investigation of this phenomenon is warranted.

Table 1
Summary of friction velocity thresholds, $u_{*c}$ ($m\,s^{-1}$), and the corresponding rates of increase of whole-ecosystem respiration over a 10 K increase in temperature, $Q_{10}$

| Forest type | $u_{*c}$ | $Q_{10}$ | Reference |
|---|---|---|---|
| Aspen | 0.6 | 5.5 | Black et al. (1996) |
| Pine | 0.5 | 2.6 | Lindroth et al. (1998) |
| Maple-tulip poplar | 0.5 | 1.9 | Schmid et al. (2000) |
| Black spruce | 0.4 | 2.0 | Jarvis et al. (1997) |
| Douglas-fir | 0.4 | 4.5 | Jork et al. (1998) |
| Beech | 0.25 | 3.0 | Pilgaard et al. (2001) |
| Black spruce | 0.2 | 2.0 | Goulden et al. (1997) |
| Oak-maple | 0.17 | 2.1 | Goulden et al. (1996) |
| Spruce-hemlock | 0.15 | 2.4 | Hollinger et al. (1999) |
| Maple-aspen | 0.15 | 2.9 | Lee et al. (1999) |
| Tropical | 0.0 | NA[a] | Malhi et al. (1998) |

[a] Not available.

Causes of nighttime flux underestimation remain the subject of debate. Poor instrument response at high frequencies contributes to the flux loss, but is unlikely the root of the problem because the flux will be still be too low even using the large correction factors predicted for the stable conditions (Massman 2000, 2001). We conclude that the problem is meteorological in nature and recommend an experiment that simultaneously measures all the terms of the mass conservation equations [Eqs. (6) and (8)]—an admittedly difficult task. Drainage flow is one possible reason why fluxes measured under very stable stratification always seem biased toward underestimation (Grace et al., 1996; Lee, 1998). This raises the possibility that $CO_2$ fluxes from low areas that accumulate $CO_2$ from drainage must be relatively high to compensate. Such high fluxes have yet to be observed. Studies of the influence of drainage flows on trace gas movement are strongly encouraged.

## 7. Summary and recommendations

The findings of this study and areas needing further research are:

(1) *The pressure covariance term*: $\overline{\mathbf{v}' p'_a}$. Although usually ignored, the pressure covariance component of the WPL term (Webb et al., 1980) is likely to be important during windy turbulent conditions. Ignoring this term could lead to a significant bias at sites that have frequent high winds and strong turbulence.

(2) *The quasi-advective term*: $\overline{\mathbf{v}' \rho'_d} \cdot \nabla \bar{\omega}_c - \mathbf{V} \bar{\omega}_c \cdot \nabla \bar{\rho}_d$. We have identified a new (or previously unidentified) term in the $CO_2$ budget equations, Eqs. (6) and (18), which we have termed the quasi-advective term. This term originates from the 3D dry air density correction (Paw U et al., 2000, Appendix B). The significance of this term to long-term $CO_2$ eddy covariance studies is unknown. But, it is suggested that this term is likely to be important anywhere that within-canopy gradients of $CO_2$ mass mixing ratio, $\nabla \bar{\omega}_c$, and the profiles of temperature covariance, $\overline{\mathbf{v}' T'_a}/\bar{T}_a$, water vapor covariance, $\overline{\mathbf{v}' \rho'_v}/\bar{\rho}_v$, and pressure covariance, $\overline{\mathbf{v}' p'_a}/\bar{p}_a$, are important.

(3) *Methods for correcting frequency attenuation*. Two methods of correcting eddy covariances for spectral attenuation are reviewed and analyzed. The low-pass filter method (Goulden et al., 1997; Hollinger et al., 1999) has a potentially significant advantage over the analytical method (Massman, 2000, 2001) for high frequency cospectral attenuation because it is independent of cospectral shape. The analytical method, on the other hand, does include some high frequency attenuation factors related to phase shifts that are not part of the low-pass filter method. The analytical method also incorporates low frequency attenuation which is not included in the low-pass filter method. This last difference between the two spectral correction methods further highlights the importance of the loss of low frequency cospectral power as a potentially significant source of error for long-term flux and energy balances (Högström, 2000; Sakai et al., 2001; Finnigan et al., 2002). Neither spectral correction method is entirely satisfactory for very stable conditions. Nevertheless, a detailed quantitative comparison of the two methods and their impacts on long-term fluxes has yet to be performed and further investigations into low frequency issues and very stable conditions are necessary.

(4) *2D and 3D effects*. Advective effects are a major source of uncertainty, particularly in complex terrain, and they may not be fully quantified without the aid of 2D and 3D models. However, drainage flows are likely to be amenable to observational studies and more studies of $CO_2$ drainage should be performed.

(5) *Coordinate systems*. Choice of a coordinate system is quite important. For example, processing flux data with the 'natural' (Tanner and Thurtell, 1969) or 'streamline' (Wilczak et al., 2001) coordinate system may cause the loss of the vertical advective component of the flux (because $W = 0$ in the natural coordinate system) and remove some of the low frequency contribution to the fluxes (Finnigan et al., 2002). Consequently, other coordinate systems, most notably the planar fit method of Wilczak et al. (2001) and Paw U et al. (2000), should be investigated and their impact on long-term flux and energy should be quantified. We also note that when writing a budget equation in any particular coordinate system it is important to use the 3D form of the coordinate system first and then to simplify to the 1D case as necessary, and finally, where possible, measure or account for all terms in the budget equation.

(6) *Nighttime and low flux issues*. Many of the previously discussed shortcomings of eddy covariance technology coincide when attempting flux measurements at night. Spectral correction methods are unreliable or questionable, drainage is more likely to occur during relatively stable nighttime conditions, and turbulent transfer may become intermittent in time and space. There are other issues or phenomena that further confound flux measurements made at night. The presence of shear-generated traveling gravity waves trapped in near-surface atmospheric stable layers invalidate the constant flux layer assumption. One practical method for estimating nighttime fluxes employs data filling during periods of low turbulence using a $u_*$ threshold. However, it is now recognized that this approach is relatively site specific. Further complicating both nighttime and daytime issues is the possibility that atmospheric pressure pumping may augment or reduce soil diffusive $CO_2$ efflux particularly over rough topography. Such an effect raises some uncertainty

in $Q_{10}$-based algorithms developed for nighttime data filling because these algorithms assume that biological source strength is independent of turbulence and pressure pumping. We conclude that the difficulties of making nighttime flux measurements are largely meteorological in nature, not instrumental. To insure further progress on these nighttime flux issues and the other previously discussed issues more research is needed into how gravity waves, intermittency, drainage, and pressure pumping affect flux measurements.

## Acknowledgements

This workshop was supported by grant 901214-HAR from the US DOE NIGEC Northeast Regional Center. The second author also acknowledges support by the US National Science Foundation through grants ATM-9629497 and ATM-0072864. Both authors wish to thank Jielun Sun, Don Lenschow, and an anonymous reviewer for their comments and insights on the subjects covered by this study.

## Appendix A. The UFO committee and Participants of the UFO workshop

This appendix is an alphabetical list of the participants of the workshop for unaccounted flux in long-term studies of carbon and energy exchanges (UFO). Those participants whose names are marked with ∗ are members of the UFO committee. The invited speakers are denoted by †. The workshop was co-chaired by Bill Massman and Xuhui Lee.

Dean Anderson
Peter Anthoni
Marc Aubinet
Dennis Baldocchi∗
Brad Berger
Constance Brown-Mitic
George Burba
Robert Clement
Ken Davis
John Finnigan†
David Fitzjarrald†
John Frank
Michael Goulden∗†
Lianhong Gu
Jeffrey Hare
Dave Hollinger∗
Thomas Horst†
Larry Jacobsen
Gabriel Katul
Xuhui Lee∗
Don Lenschow
Ray Leuning
Yadvinder Mahli†
Larry Mahr
Bill Massman∗†
Russel Monson
Steve Oncley
Kyaw Tha Paw U
Üllar Rannik
Ruth Reck†
Luis Ribeiro
Scott Saleska
HaPe Schmidt
Jielun Sun
Andy Suyker
Bert Tanner
Andy Turnipseed
Sashi Verma∗
Marv Wesely
Eric Williams
Steve Wofsy∗†

## Appendix B. Derivation of the fundamental equations of eddy covariance

This appendix derives and discusses the fundamental eddy covariance equations for the measurement of the fluxes of water vapor, heat and $CO_2$, Eqs. (2)–(6) of the main text. These equations are derived in a fully consistent manner with the minimum number of assumptions and include temperature, pressure, and moisture effects and generalize the results of Webb et al. (1980) (WPL) and Paw U et al. (2000). Expansion of all requisite equations with respect to the perturbation fields follows WPL, but also include pressure effects. However, unlike WPL, we keep only the first-order (linear) terms in the perturbation fields in accordance with the findings of Fuehrer and Friehe

(2002). To allow for the possibility of horizontal advection, we employ the general 3D mass conservation for dry air (Paw U et al., 2000) when deriving the WPL term, rather than assume the net mean vertical dry air mass flux is zero, as do WPL. Furthermore, we expand on previous studies by deriving an explicit relationship between the source terms for dry air and $CO_2$. Finally, we note that, although we focus on $CO_2$, the method outlined here is generalizable to all other trace gases as well.

### *B.1. Trace gas fluxes*

This discussion begins by listing the key equations on which the derivation for trace gas fluxes is based.

The total density of the atmosphere, $\rho_a$, is the sum of dry and vapor components, i.e.,

$$\rho_a = \rho_d + \rho_v \tag{B.1}$$

where, henceforth, $\rho$ denotes density, the subscript 'a' denotes ambient or total, the subscript 'd' denotes the dry air component, the subscript 'v' denotes the vapor component, and where necessary, the subscript 'c' denotes the trace gas component, which in this case will be taken to be $CO_2$.

Dalton's law of partial pressure is

$$p_a = p_d + p_v \tag{B.2}$$

where $p$ denotes pressure.

The ideal gas laws for the three constituents and the ambient air are

$$p_d = \frac{\rho_d R T_a}{m_d} \tag{B.3}$$

$$p_v = \frac{\rho_v R T_a}{m_v} \tag{B.4}$$

$$p_c = \frac{\rho_c R T_a}{m_c} \tag{B.5}$$

$$p_a = \frac{\rho_a R T_a}{m_a} \tag{B.6}$$

where $T_a$ is the ambient temperature, $R$ the universal gas constant and $m$ the molecular mass of the gas as indicated by the subscript.

By ignoring molecular diffusion, the conservation of mass, or the equation of continuity, for $CO_2$ and dry air are

$$\frac{\partial \rho_c}{\partial t} + \nabla \cdot (\mathbf{v}\rho_c) = S_c \tag{B.7}$$

$$\frac{\partial \rho_d}{\partial t} + \nabla \cdot (\mathbf{v}\rho_d) = S_d \tag{B.8}$$

where vectors are denoted in bold type, $\nabla$ is the spatial gradient operator, $\mathbf{v}$ the velocity and the subscripted $S$ the corresponding source or sink term. It should also be emphasized that equations of continuity, Eqs. (B.7) and (B.8), are expressed in 3D vector form and are, therefore, independent of any assumptions regarding horizontal gradients or any particular coordinate system.

For the purposes of the present discussion, which we limit to photosynthesis and respiration, the source term for dry air, $S_d$, can be expressed in terms of $S_c$. The coupling between $O_2$ and $CO_2$ is such that for every mole of one gas used during photosynthesis or respiration a mole of the other is created, i.e., $S_{O_2}/m_{O_2} = -S_c/m_c$, where $S_{O_2}$ is the source strength of $O_2$ and $m_{O_2}$ is the molecular mass of $O_2$. As long as these processes do not significantly alter the basic composition of dry air, we m ay also assume that $S_c + S_{O_2} = S_d$. Therefore we can make the following substitution for $S_d$ in Eq. (B.8): $S_d = (1 - (m_{O_2}/m_c))S_c$.

Before formally manipulating this set of equations, we need to define two more terms. The $CO_2$ mass mixing ratio (or $CO_2$ mass fraction), $\omega_c$, and the $CO_2$ volume mixing ratio (or $CO_2$ mole fraction or $CO_2$ volume fraction), $\chi_c$, are given as follows:

$$\omega_c = \frac{\rho_c}{\rho_d} \tag{B.9}$$

$$\chi_c = \frac{p_c}{p_d} \tag{B.10}$$

Assuming the $CO_2$ and dry air components are isothermal, the relationship between $\omega_c$ and $\chi_c$ is $\omega_c = (m_c/m_d)\chi_c$. Similar relationships can be defined for water vapor.

Combining Eqs. (B.1)–(B.6), yields

$$\frac{\rho_d}{m_d} + \frac{\rho_v}{m_v} = \frac{p_a}{R T_a} \tag{B.11}$$

Performing the Reynolds's decomposition on Eqs. (B.7)–(B.11), yields the following four equations

$$\bar{\omega}_c = \frac{\bar{\rho}_c}{\bar{\rho}_d} = \frac{m_c}{m_d}\bar{\chi}_c = \frac{1}{\mu_c}\frac{\bar{p}_c}{\bar{p}_d} \tag{B.12}$$

$$\rho_{\mathrm{d}}' = -\bar{\rho}_{\mathrm{d}}(1+\bar{\chi}_{\mathrm{v}})\left[\delta_{\mathrm{oc}}\frac{T_{\mathrm{a}}'}{\bar{T}_{\mathrm{a}}} - \frac{p_{\mathrm{a}}'}{\bar{p}_{\mathrm{a}}}\right] - \mu_{\mathrm{v}}\rho_{\mathrm{v}}' \qquad \text{(B.13)}$$

$$\frac{\partial\bar{\rho}_{\mathrm{c}}}{\partial t} + \nabla\cdot(\mathbf{V}\bar{\rho}_{\mathrm{c}} + \overline{\mathbf{v}'\rho_{\mathrm{c}}'}) = \bar{S}_{\mathrm{c}} \qquad \text{(B.14)}$$

$$\frac{\partial\bar{\rho}_{\mathrm{d}}}{\partial t} + \nabla\cdot(\mathbf{V}\bar{\rho}_{\mathrm{d}} + \overline{\mathbf{v}'\rho_{\mathrm{d}}'}) = \left(1 - \frac{m_{\mathrm{O_2}}}{m_{\mathrm{c}}}\right)\bar{S}_{\mathrm{c}} \qquad \text{(B.15)}$$

where $\mu_{\mathrm{c}} = m_{\mathrm{d}}/m_{\mathrm{c}}$, $\mu_{\mathrm{v}} = m_{\mathrm{d}}/m_{\mathrm{v}}$, the mean wind is denoted by $\mathbf{V}$ rather than denoting it with the overbar notation, and all deviation quantities (here and henceforth) are denoted by $'$. Note that all products in the deviation quantities were dropped from Eqs. (B.12) and (B.13) and that Eq. (B.13) has been linearized in the deviation quantities similar to Webb et al. (1980). Finally $\delta_{\mathrm{oc}}$ is introduced in the $T_{\mathrm{a}}'$ term of Eq. (B.13) to distinguish between open- and closed-path sensors. For an open-path sensor $\delta_{\mathrm{oc}} = 1$ and for a closed-path sensor $\delta_{\mathrm{oc}} = 0$. For closed-path systems, $\delta_{\mathrm{oc}} = 0$ because by the time the gas sample has reached the analyzer the temperature fluctuations have been attenuated so strongly by the sampling tube that they can probably be ignored (Frost, 1981; Leuning and Moncrieff, 1990; Rannik et al., 1997). This distinction between open- and closed-path sensors relative to the fluctuations in density, $\rho_{\mathrm{d}}'$, and its implications to eddy covariance measurements are discussed in more detail in the main text.

Next multiplying Eq. (B.15) by $\bar{\omega}_{\mathrm{c}}$, subtracting the result from Eq. (B.14), and then manipulating the terms algebraically yields:

$$\begin{aligned}\bar{\rho}_{\mathrm{d}}\frac{\partial\bar{\omega}_{\mathrm{c}}}{\partial t} &+ [\overline{\mathbf{v}'\rho_{\mathrm{d}}'}\cdot\nabla\bar{\omega}_{\mathrm{c}} - \mathbf{V}\bar{\omega}_{\mathrm{c}}\cdot\nabla\bar{\rho}_{\mathrm{d}}] \\ &+ \nabla\cdot(\mathbf{V}\bar{\rho}_{\mathrm{c}} + \overline{\mathbf{v}'\rho_{\mathrm{c}}'} - \bar{\omega}_{\mathrm{c}}\overline{\mathbf{v}'\rho_{\mathrm{d}}'}) \\ &= \left[1 + \left(\frac{m_{\mathrm{O_2}}}{m_{\mathrm{c}}} - 1\right)\bar{\omega}_{\mathrm{c}}\right]\bar{S}_{\mathrm{c}} \qquad \text{(B.16)}\end{aligned}$$

This is the fundamental equation of continuity for in situ measurements of $CO_2$ fluxes and background concentrations using one or more eddy covariance sensors that directly measure fluctuations in density. Mathematically Eq. (B.16) is not unique, i.e., it can be written in other ways. But, expressing Eq. (B.16) as we have aids in the interpretation of the WPL term. In traditional applications, the WPL term is applied solely to fluxes measured at a single level. Therefore, we include the dry air flux term, $-\bar{\omega}_{\mathrm{c}}\overline{\mathbf{v}'\rho_{\mathrm{d}}'}$, as part of the total flux, $\mathbf{V}\bar{\rho}_{\mathrm{c}} + \overline{\mathbf{v}'\rho_{\mathrm{c}}'} - \bar{\omega}_{\mathrm{c}}\overline{\mathbf{v}'\rho_{\mathrm{d}}'}$. This, in turn, emphasizes that the dry air or density effects have a 3D aspect, expressed by the term $[\overline{\mathbf{v}'\rho_{\mathrm{d}}'}\cdot\nabla\bar{\omega}_{\mathrm{c}} - \mathbf{V}\bar{\omega}_{\mathrm{c}}\cdot\nabla\bar{\rho}_{\mathrm{d}}]$, that Webb et al. (1980) did not include. In other words, WPL did not specifically include the within-surface layer effects associated with vertical and horizontal structure of the fluxes and mean density of dry air. In a 1D setting, we could state that the dry air density fluctuations influence, not only the vertical trace gas fluxes, but that they extend throughout the surface layer and can influence exchanges below the level of flux measurement. A second difference between the present approach and WPL is the use of the continuity equation for dry air, Eq. (B.15). WPL assume that the 1D dry air flux, $W\bar{\rho}_{\mathrm{d}} + \overline{w'\rho_{\mathrm{d}}'} = 0$. In doing so, their $W$ becomes a drift velocity and it loses the interpretation of a mean flow velocity appropriate to atmospheric flows. This is an important distinction for applications where the fluxes are rotated into a coordinate system that allows for $W \neq 0$. In this case, $W$ is a mean vertical velocity associated with atmospheric or topographic forcing independent of any dry air flux. Nevertheless, it is important to recognize that if the point measurement of $CO_2$ fluxes is the only concern, then the present results are the same as WPL. But, if an accurate accounting of the aerodynamic budget for $CO_2$ is the main goal, then Eq. (B.16), is more appropriate. The only situation where Eq. (B.16) and the original WPL tend to correspond with one another is when $\overline{\mathbf{v}'\rho_{\mathrm{d}}'}\cdot\nabla\bar{\omega}_{\mathrm{c}} \equiv \mathbf{V}\bar{\omega}_{\mathrm{c}}\cdot\nabla\bar{\rho}_{\mathrm{d}}$, which seems unlikely at best.

Several other points need to be noted here regarding this equation. First, the incompressibility assumption for the mean flow ($\nabla\cdot\mathbf{V} = 0$) has been employed in the derivation of Eq. (B.16), otherwise the term $-\mathbf{V}\bar{\omega}_{\mathrm{c}}\cdot\nabla\bar{\rho}_{\mathrm{d}}$ should be replaced by $\bar{\omega}_{\mathrm{c}}\nabla\cdot\mathbf{V}\bar{\rho}_{\mathrm{d}}$. Second, Paw U et al. (2000) derive a related 1D version of this equation. Third (discussed below), Eq. (B.16) is not necessarily correct for in situ flux measurements based on the mixing ratio fluctuations $\omega_{\mathrm{c}}'$ or $\chi_{\mathrm{c}}'$. Fourth, greater mathematical precision is possible, particularly concerning issues involving horizontal variability, when developing a budget equation like Eq. (B.16) by first defining a control volume of some horizontal extent and then beginning that development by integrating Eq. (B.16) over that control volume (e.g., Finnigan, personal communication). But such precision is not necessary for the present study, because the insights

offered by this more complete approach are fully covered by Finnigan (personal communication). Finally, we note that because $((m_{O_2}/m_c)-1)\bar{\omega}_c \ll 1$, it is not be included in the main text, but, for the purposes of completeness, it is kept in this appendix.

The interpretation of the three terms on the left-hand side of this equation is fairly standard, even if the explicit form is not. The first term is the time rate of change term. The second term, $[\overline{\mathbf{v}'\rho_d'}\cdot\nabla\bar{\omega}_c - \mathbf{V}\bar{\omega}_c\cdot\nabla\bar{\rho}_d]$, is a quasi-advective term and the third is the flux divergence term. From this third term, the appropriate trace gas flux, $\mathbf{F}_c$, can be identified; $\mathbf{F}_c = \mathbf{V}\bar{\rho}_c + \overline{\mathbf{v}'\rho_c'} - \bar{\omega}_c\overline{\mathbf{v}'\rho_d'}$, which when combined with Eqs. (B.1), (B.12) and (B.13) yields:

$$\mathbf{F}_c = \mathbf{V}\bar{\rho}_c + \overline{\mathbf{v}'\rho_c'} + \bar{\rho}_c(1+\bar{\chi}_v)\left[\delta_{oc}\frac{\overline{\mathbf{v}'T_a'}}{\bar{T}_a} - \frac{\overline{\mathbf{v}'p_a'}}{\bar{p}_a}\right] + \bar{\omega}_c\mu_v\overline{\mathbf{v}'\rho_v'} \tag{B.17}$$

Note that Eq. (B.17) explicitly includes the pressure covariance term, $\overline{\mathbf{v}'p_a'}/\bar{p}_a$, which WPL did not. Under most circumstances involving water vapor and $CO_2$ fluxes, this term is probably small enough to ignore, however, as discussed in the main text, there are situations where the pressure covariance term could be significant.

While the interpretation of Eq. (B.16) may be routine, the implications are potentially significant and result from the quasi-advective term. This can be seen by noting that budget equations for trace gases developed by vertically integrating equations similar to Eq. (B.16) (e.g., Moncrieff et al., 1996; Lee, 1998, and others) usually do not include the quasi-advective term. Eq. (B.16) indicates that applications of mass flux term requires not only augmentation of the measured $CO_2$ covariance $\overline{\mathbf{v}'\rho_c'}$ with $-\bar{\omega}_c\overline{\mathbf{v}'\rho_d'}$, but knowledge of the vertical profiles of components of $\overline{\mathbf{v}'\rho_d'}$ as well. Consequently, there is the potential for some inaccuracies in the current calculations of the vertically integrated $CO_2$ budgets and the inferred NEE.

One benefit of the present formalism for developing the WPL term for trace gas exchange is that it readily adapts to the inclusion of two instrument related corrections: the correction to $CO_2$ fluctuations due to sensor sensitivity to water vapor (Leuning and Moncrieff, 1990) and the oxygen (or $O_2$) correction to water vapor fluctuations measured with a Krypton Hygrometer (Tanner et al., 1993). These corrections are summarized below in two sets of equations. The first set, Eqs. (B.18) and (B.19), is for the complete (or symmetric, but rather unlikely) case of measuring the $CO_2$ flux with one sensor and the water vapor flux with a Krypton Hygrometer:

$$\rho_v'\{\text{corrected}\} = \rho_v'\{K\,H_2O\} + \gamma\bar{\rho}_{O_2}\left[\frac{T_a'}{\bar{T}_a} - \frac{p_a'}{\bar{p}_a}\right] \tag{B.18}$$

$$\rho_c'\{\text{corrected}\} = \rho_c'\{\text{raw}\} - \frac{\alpha}{\beta}\rho_v'\{K\,H_2O\} - \frac{\alpha}{\beta}\gamma\bar{\rho}_{O_2}\left[\frac{T_a'}{\bar{T}_a} - \frac{p_a'}{\bar{p}_a}\right] \tag{B.19}$$

The more likely scenario, measuring both water vapor and $CO_2$ fluctuations with a single instrument, is given by the following equations:

$$\rho_v'\{\text{corrected}\} = \rho_v'\{\text{raw}\} \tag{B.20}$$

$$\rho_c'\{\text{corrected}\} = \rho_c'\{\text{raw}\} - \frac{\alpha}{\beta}\rho_v'\{\text{raw}\} \tag{B.21}$$

where $\alpha/\beta \le 10^{-3}$, $\gamma \approx 0.05$ (Tanner et al., 1993), and $\bar{\rho}_{O_2}$ is the ambient concentration of $O_2$ [kg m$^{-3}$]. (Note $\bar{\rho}_{O_2} = 0.23\bar{\rho}_d$.) These corrections apply to both the concentration flux, $\overline{\mathbf{v}'\rho_c'}$, and the mass flux term, $\overline{\mathbf{v}'\rho_d'}$, of Eqs. (B.16) and (B.17), where the 'corrected' fluctuations replace the 'raw' or 'uncorrected' quantities in Eqs. (B.13)–(B.17).

We end this section of this appendix by citing (without proof) the fundamental equation of eddy covariance for in situ flux measurements based on mixing ratio, $\omega_c'$ or $\chi_c'$. It is

$$\bar{\rho}_d\frac{\partial\bar{\omega}_c}{\partial t} + [\overline{\mathbf{v}'\rho_d'}\cdot\nabla\bar{\omega}_c - \mathbf{V}\bar{\omega}_c\cdot\nabla\bar{\rho}_d] + \nabla\cdot(\mathbf{V}\bar{\rho}_d\bar{\omega}_c + \bar{\rho}_d\overline{\mathbf{v}'\omega_c'}) = \left[1+\left(\frac{m_{O_2}}{m_c}-1\right)\bar{\omega}_c\right]\bar{S}_c \tag{B.22}$$

The derivation of this equation follows from substituting $\mathbf{v}\rho_d\omega_c$ for $\mathbf{v}\rho_c$ in the divergence term of Eq. (B.7) and then employing the same assumptions and general approach used to derive Eq. (B.16). Eq. (B.22) is in agreement with the results of Webb et al. (1980) in that no additional covariance

term is required when estimating the total flux, because it is measured directly as $\bar{\rho}_d\overline{\mathbf{v}'\omega_c'}$. However, it should also be noted that the quasi-advective term, $[\overline{\mathbf{v}'\rho_d'}\cdot\nabla\bar{\omega}_c - \mathbf{V}\bar{\omega}_c\cdot\nabla\bar{\rho}_d]$, remains part of this form of the continuity equation.

### B.2. Turbulent temperature flux: $\overline{\mathbf{v}'T_a'}$

Eqs. (B.13), (B.16) and (B.17) clearly indicate the importance of the ambient temperature flux, $\overline{\mathbf{v}'T_a'}$, to the WPL term of the water vapor and $CO_2$ fluxes. However, modern sonic thermometry does not directly measure the ambient temperature, $T_a$, or the turbulent fluctuations $T_a'$ (Kaimal and Gaynor, 1991). Rather, modern sonics measure the sonic virtual temperature, $T_s$, defined by Kaimal and Gaynor (1991) as $T_a(1+0.32p_v/p_a)$. This section derives the relationship between $\mathbf{v}'T_s'$ and $\overline{\mathbf{v}'T_a'}$.

Assuming the definition of $T_s$ just given, we first decompose $T_s$ into a mean, $\bar{T}_s$, and a fluctuating component, $T_s'$ and then perform the Reynolds averaging on the resulting equation. This yields the following two equations:

$$\bar{T}_s = \bar{T}_a(1+\bar{\sigma}_v) \tag{B.23}$$

$$T_s' = T_a'(1+\bar{\sigma}_v) + \bar{\sigma}_v\bar{T}_a\left[\frac{\rho_v'}{\bar{\rho}_v} - \frac{p_a'}{\bar{p}_a}\right] \tag{B.24}$$

where $\bar{\sigma}_v = (0.32\bar{p}_v/\bar{p}_a)$. For this derivation we have (i) taken advantage of Eq. (B.4) to simplify $p_v'$, (ii) ignored the small cross-correlation terms in Eq. (B.23), and (iii) linearized Eq. (B.24) in the $p_a'/\bar{p}_a$ term. Multiplying Eq. (B.24) by $\mathbf{v}'$ and taking the Reynolds average of the resulting equation yields the following equation for the turbulent temperature flux, $\overline{\mathbf{v}'T_a'}$.

$$\overline{\mathbf{v}'T_a'} = \frac{\overline{\mathbf{v}'T_s'}}{1+\bar{\sigma}_v} - \frac{\bar{\sigma}_v}{1+\bar{\sigma}_v}\bar{T}_a\left[\frac{\overline{\mathbf{v}'\rho_v'}^F}{\bar{\rho}_v} - \frac{\overline{\mathbf{v}'p_a'}}{\bar{p}_a}\right] \tag{B.25}$$

Dividing both sides of this equation by $\bar{T}_a$ and simplifying the ratio $\bar{\sigma}_v/\bar{\rho}_v$ for the vapor flux term and $\bar{\sigma}_v/(1+\bar{\sigma}_v)$ for the pressure flux term yields the following (more computationally useful) equation:

$$\frac{\overline{\mathbf{v}'T_a'}}{\bar{T}_a} = \frac{\overline{\mathbf{v}'T_s'}}{\bar{T}_s} - \bar{\alpha}_v\frac{\overline{\mathbf{v}'\rho_v'}^F}{\bar{\rho}_d} + \bar{\beta}_v\frac{\overline{\mathbf{v}'p_a'}}{\bar{p}_a} \tag{B.26}$$

where $\bar{\alpha}_v = 0.32\mu_v/(1+1.32\bar{\chi}_v)$ and $\bar{\beta}_v = 0.32\bar{\chi}_v/(1+1.32\bar{\chi}_v)$.

In addition to the vapor correction ($\overline{\mathbf{v}'\rho_v'}^F$ and $\overline{\mathbf{v}'p_a'}$ terms), it may also be necessary to correct the sonic virtual heat flux, $\overline{\mathbf{v}'T_s'}$, for cross-wind effects (e.g., Kaimal and Gaynor, 1991; Hignett, 1992). Including this correction term in Eq. (B.26) yields

$$\frac{\overline{\mathbf{v}'T_a'}}{\bar{T}_a} = \frac{\overline{\mathbf{v}'T_s'}}{\bar{T}_s} - \bar{\alpha}_v\frac{\overline{\mathbf{v}'\rho_v'}^F}{\bar{\rho}_d} + \bar{\beta}_v\frac{\overline{\mathbf{v}'p_a'}}{\bar{p}_a} + \delta_{un}\frac{2U_n\overline{u_n'\mathbf{v}'}}{\gamma_d R_d\bar{T}_s} \tag{B.27}$$

where $\gamma_d R_d = 402\,\mathrm{m^2\,s^{-2}\,K^{-1}}$, $U_n$ and $u_n'$ are the mean wind speed ($U_n$) and the wind speed fluctuations ($u_n'$) normal to the axis of the sonic that measures temperature (usually the $w'$ axis), and $\delta_{un}$ is 0 if the sonic's internal signal processing software includes this correction and 1 if it does not. We do not consider this correction any further in this study because some sonics already include this correction internally in their signal processing software. But, because we are uncertain whether all sonics include this correction or not, we feel it important to point out the existence of these cross-wind effects. For example, for most applications the vertical component of this term is proportional to $U\overline{u'w'}$, which implies that it should not be ignored during windy or very turbulent conditions.

### B.3. The combined turbulent fluxes

Eq. (B.26) indicates that $\overline{\mathbf{v}'T_a'}$ measured using sonic thermometry is a function of the water vapor flux. However, as indicated in Section B.1, the vapor flux, $\overline{\mathbf{v}'\rho_v'}^F$, must include the WPL term, which in turn is a function of $\overline{\mathbf{v}'T_a'}$. Therefore, the temperature and vapor flux expressions form coupled equations. We complete this section by combining the results of the two previous sections stating the solution for $\overline{\mathbf{v}'T_a'}$ and the resulting expressions for $\overline{\mathbf{v}'\rho_v'}^F$ and $CO_2$, $\overline{\mathbf{v}'\rho_c'}^F$. For the present purposes, none of these fluxes include the mean flow component.

$$\frac{\overline{\mathbf{v}'T_a'}}{\bar{T}_a} = \left[\frac{1}{1+\delta_{oc}\bar{\lambda}_v}\right]\frac{\overline{\mathbf{v}'T_s'}}{\bar{T}_s} - \left[\frac{\bar{\alpha}_v(1+\bar{\chi}_v)}{1+\delta_{oc}\bar{\lambda}_v}\right]\frac{\overline{\mathbf{v}'\rho_v'}}{\bar{\rho}_d} + \left[\frac{\bar{\beta}_v(2+\bar{\chi}_v)}{1+\delta_{oc}\bar{\lambda}_v}\right]\frac{\overline{\mathbf{v}'p_a'}}{\bar{p}_a} \tag{B.28}$$

$$\overline{\mathbf{v}'\rho_v'}^{F} = (1+\bar{\chi}_v)\overline{\mathbf{v}'\rho_v'} + \bar{\rho}_v(1+\bar{\chi}_v) \times \left[\delta_{oc}\frac{\overline{\mathbf{v}'T_a'}}{\bar{T}_a} - \frac{\overline{\mathbf{v}'p_a'}}{\bar{p}_a}\right] \quad \text{(B.29)}$$

$$\overline{\mathbf{v}'\rho_c'}^{F} = \overline{\mathbf{v}'\rho_c'} + \bar{\rho}_c(1+\bar{\chi}_v)\left[\delta_{oc}\frac{\overline{\mathbf{v}'T_a'}}{\bar{T}_a} - \frac{\overline{\mathbf{v}'p_a'}}{\bar{p}_a}\right] + \bar{\omega}_c\mu_v\overline{\mathbf{v}'\rho_v'} \quad \text{(B.30)}$$

where $\bar{\lambda}_v = \bar{\beta}_v(1+\bar{\chi}_v)$ and $\bar{\alpha}_v\bar{\omega}_v = \bar{\beta}_v$. By convention, Eq. (B.28) expresses $\overline{\mathbf{v}'T_a'}$ in terms of the covariances between the sonic anemometer and the instruments used to measure vapor and pressure fluctuations. Once $\overline{\mathbf{v}'T_a'}$ has been determined from Eq. (B.28), it then can be used in Eqs. (B.29) and (B.30) to estimate the fluxes of water vapor and other trace gases.

In summary, in the main text we cite Eqs. (B.16), (B.17), (B.28)–(B.30) and its equivalent for water vapor, and the WPL or dry air flux equation, the equation for $\overline{\mathbf{v}'\rho_d'}$ estimated from Eq. (B.13), as the fundamental equations of eddy covariance.

### *B.4. The turbulent heat flux*

For the sake of completeness, Eq. (B.31) below gives the turbulent 3D heat flux, **H**, in terms of the temperature flux, $\overline{\mathbf{v}'T_a'}$, and is adapted from Sun et al. (1995):

$$\mathbf{H} = [\bar{\rho}_d C_{pd} + \bar{\rho}_v C_{pv}]\overline{\mathbf{v}'T_a'} \quad \text{(B.31)}$$

where $C_{pd}$ is the specific heat capacity for dry air ($=1005\,\mathrm{J\,kg^{-1}\,K^{-1}}$) and $C_{pv}$ is the specific heat capacity for water vapor ($=1846\,\mathrm{J\,kg^{-1}\,K^{-1}}$). Other relatively small terms (Sun et al., 1995) are negligible for the present purposes.

## References


Aubinet, M., Grelle, A., Ibrom, A., Rannik, Ü., Moncrieff, J., Foken, T., Kowalski, A.S., Martin, P.H., Berbigier, P., Bernhofer, C., Clement, R., Elbers, J., Granier, A., Grunwald, T., Morgenstern, K., Pilegaard, K., Rebmann, C., Snijders, W., Valentini, R., Vesala, T., 2000. Estimates of the annual net carbon and water exchange of forests: the EUROFLUX methodology. Adv. Ecol. Res. 30, 113–175.

Baldocchi, D.D., Meyers, T.P., 1991. Trace gas exchange above the forest floor of a deciduous forest. 1. Evaporation and $CO_2$ efflux. J. Geophys. Res. 96, 7271–7285.

Baldocchi, D., Finnigan, J., Wilson, K., Paw U, K.T., Falge, E., 2000. On measuring net ecosystem carbon exchange over tall vegetation on complex terrain. Bound.-Lay. Meteorol. 96, 257–291.

Barr, A.G., Griffis, T., Black, T.A., Lee, X., Staebler, R.M., Fuentes, J.D., Chen, Z., Morgenstern, K., 2002. Comparing the carbon budgets of mature boreal and temperate deciduous forest stands. Can. J. For. Res. 32, 813–822.

Berger, B.W., Davis, K.J., Yi, C., Bakwin, P.S., Zhao, C.L., 2001. Long-term carbon dioxide fluxes from a very tall tower in a northern forest: flux measurement methodology. J. Atmos. Ocean. Technol. 18, 529–542.

Black, T.A., den Hartog, G., Neumann, H.H., Blanken, P.D., Yang, P.C., Russell, C., Nesic, Z., Lee, X., Chen, S.G., Staebler, R., Novak, M.D., 1996. Annual cycles of water vapor and carbon dioxide fluxes in and above a boreal aspen forest. Glob. Change Biol. 2, 219–229.

Black, T.A., Chen, W.J., Barr, A.G., Arain, M.A., Chen, Z., Nesic, Z., Hogg, E.H., Neumann, H.H., Yang, P.C., 2000. Increased carbon sequestration by a boreal deciduous forest in years with a warm spring. Geophys. Res. Lett. 27, 1271–1274.

Brost, R.A., Wyngaard, J.C., 1978. A model study of the stably stratified planetary boundary layer. J. Atmos. Sci. 35, 1427–1440.

Colbeck, S.C., 1989. Air movement in snow due to wind pumping. J. Glaciol. 35, 209–213.

Dyer, A.J., 1963. The adjustment of profiles and eddy fluxes. Quart. J. R. Meteorol. Soc. 89, 276–280.

Eugster, W., Senn, W., 1995. A cospectral correction model for measurement of turbulent $NO_2$ flux. Bound.-Lay. Meteorol. 74, 321–340.

Farrell, D.A., Graecen, E.L., Gurr, C.G., 1966. Vapor transfer in soil due to air turbulence. Soil Sci. 102, 305–313.

Finnigan, J., 1983. A streamline coordinate system for distorted turbulent shear flows. J. Fluid Mech. 130, 241–258.

Finnigan, J., 1999. A comment on the paper by Lee (1998): "On micrometeorological observations of surface air-exchange over tall vegetation". Agric. For. Meteorol. 97, 55–64.

Finnigan, J., Brunet, Y., 1995. Turbulent airflow in forests on flat and hilly terrain. In: Coutts, M.P., Grace, J. (Eds.), Wind and Trees. Cambridge University Press, Cambridge, UK, pp. 3–40.

Finnigan, J.J., Clement, R., 2002. A re-evaluation of long-term flux measurement techniques. Part 2. Coordinate systems.

Finnigan, J.J., Clement, R., Mahli, Y., Leuning, R., Cleugh, H., 2002. A re-evaluation of long-term flux measurement techniques. Part 1. Averaging and coordinate rotation. Bound.-Lay. Meteorol., (in press).

Fitzjarrald, D.R., Moore, K.E., 1990. Mechanisms of nocturnal exchange between the rain forest and the atmosphere. J. Geophys. Res. 95, 16839–16850.

Frost, S.R., 1981. Temperature dispersion in turbulent pipe flow. Ph.D. Thesis. University of Cambridge, Cambridge.

Fuehrer, P.L., Friehe, C.A., 2002. Flux corrections revisited. Bound.-Lay. Meteorol. 102, 415–457.

Garratt, J.R., 1990. The internal boundary layer—a review. Bound.-Lay. Meteor. 50, 171–203.

Gash, J.H.C., Culf, A.D., 1996. Applying a linear detrend to eddy correlation data in real time. Bound.-Lay. Meteorol. 79, 301–306.

Goulden, M.L., Munger, J.W., Fan, S.-M., Daube, B.C., Wofsy, S.C., 1996. Measurements of carbon sequestration by long-term eddy covariance: methods and a critical evaluation of accuracy. Glob. Change Biol. 2, 169–182.

Goulden, M.L., Daube, B.C., Fan, S.-M., Sutton, D.J., Bazzaz, A., Munger, J.W., Wofsy, S.C., 1997. Physiological response of a black spruce forest to weather. J. Geophys. Res. 102, 28987–28996.

Grace, J., Lloyd, J., McIntyre, J., Miranda, A.C., Meir, P., Miranda, H.S., Nobre, C., Moncrieff, J., Massheder, J., Mahli, Y., Wright, I., Gash, J., 1995. Carbon dioxide uptake by an undisturbed tropical rain forest in southwest Amazonia. Science 270, 778–780.

Grace, J., Malhi, Y., Lloyd, J., McIntyre, J., Miranda, A.C., Meir, P., Miranda, H.S., 1996. The use of eddy covariance to infer the net carbon dioxide uptake of Brazilian rain forest. Glob. Change Biol. 2, 209–217.

Grelle, A., 1997. Long-term water and carbon dioxide fluxes from a boreal forest: methods and applications. Ph.D. Thesis. Swedish University of Agricultural Studies, Uppsala.

Hignett, P., 1992. Corrections to temperature measurements with a sonic anemometer. Bound.-Lay. Meteorol. 61, 175–187.

Hillel, D., 1980. Fundamentals of Soil Physics. Academic Press, New York, NY, 413 pp.

Högström, U., 2000. An alternative explanation for the systematic height variation of normalized vertical velocity variance in the near-neutral surface layer. In: Proceedings of the 14th Symposium on Boundary Layer and Turbulence. American Meteorological Society, Boston, MA, pp. 31–32.

Hollinger, D.Y., Goltz, S.M., Davidson, E.A., Lee, J.T., Tu, K., Valentine, H.T., 1999. Seasonal patterns and environmental control of carbon dioxide and water vapour exchange in an ecotonal boreal forest. Glob. Change Biol. 5, 891–902.

Horst, T.W., 1997. A simple formula for attenuation of eddy fluxes measured with first-order-response scalar sensors. Bound.-Lay. Meteorol. 82, 219–233.

Hu, X., Lee, X., Steven, D.E., Smith, R.B., 2002. A numerical study of nocturnal wavelike motion in forests. Bound.-Lay. Meteorol. 102, 199–223.

Jackson, P.S., Hunt, J.C.R., 1975. Turbulent wind flow over a low hill. Quart. J. R. Meteorol. Soc. 101, 929–995.

Jarvis, P.G., Massheder, J.M., Hale, S.E., Moncrieff, J.B., Rayment, M., Scott, S.L., 1997. Seasonal variation of carbon dioxide, water vapor, and energy exchanges of a boreal black spruce forest. J. Geophys. Res. 102, 28953–28966.

Jork, E.-M., Black, T.A., Drewitt, G.B., Humphreys, E.R., Nesic, Z., Ketler, R.J., Novak, M.D., Livingston, N.J., Spittlehouse, D.L., 1998. Long-term carbon dioxide and water vapor flux measurements above a Pacific Northwest Douglas-fir forest. In: Proceedings of the 23rd AMS Conference on Agricultural and Forest Meteorology. American Meteorological Society, Boston, MA, pp. 99–102.

Kaimal, J.C., Finnigan, J.J., 1994. Atmospheric Boundary Layer Flows—Their Structure and Measurement. Oxford University Press, New York, NY, 289 pp.

Kaimal, J.C., Gaynor, J.E., 1991. Another look at sonic thermometry. Bound.-Lay. Meteorol. 56, 401–410.

Kaimal, J.C., Wyngaard, J.C., Izumi, Y., Coté, O.R., 1972. Spectral characteristics of surface-layer turbulence. Quart. J. R. Meteorol. Soc. 98, 563–589.

Kaimal, J.C., Clifford, S.F., Lataitis, R.J., 1989. Effect of finite sampling on atmospheric spectra. Bound.-Lay. Meteorol. 47, 337–347.

Kristensen, L., 1998. Time series analysis. Dealing with imperfect data. Risø National Laboratory, Risø-I-1228(EN), 31 pp.

Kristensen, L., Fitzjarrald, D.R., 1984. The effect of line averaging on scalar flux measurements with a sonic anemometer near the surface. J. Atmos. Ocean. Technol. 1, 138–146.

Laubach, J., McNaughton, K.G., 1999. A spectrum-independent procedure for correcting eddy fluxes measured with separated sensors. Bound.-Lay. Meteorol. 89, 445–467.

Lavigne, M.B., Ryan, M.G., Anderson, D.E., Baldocchi, D.D., Crill, P.M., Fitzjarrald, D.R., Goul-den, M.L., Gower, S.T., Massheder, J.M., McCaughey, J.H., Rayment, M., Striegl, R.G., 1997. Comparing nocturnal eddy covariance measurements to estimates of ecosystem respiration made by scaling chamber measurements at six coniferous boreal sites. J. Geophys. Res. 102, 28977–28985.

Leclerc, M.Y., Thurtell, G.W., 1990. Footprint prediction of scalar fluxes using a Markovian analysis. Bound.-Lay. Meteorol. 52, 247–258.

Lee, X., 1998. On micrometeorological observations of surface-air exchange over tall vegetation. Agric. For. Meteorol. 91, 39–49.

Lee, X., 1999. Reply to comment by Finnigan on "On micrometeorological observations of surface-air exchange over tall vegetation". Agric. For. Meteorol. 97, 65–67.

Lee, X., Barr, A.G., 1998. Climatology of gravity waves in a forest. Quart. J. R. Meteorol. Soc. 124, 1403–1419.

Lee, X., Fuentes, J.D., Staebler, R., Neumann, H.H., 1999. Long-term observation of the atmospheric exchange of $CO_2$ with a temperate deciduous forest in southern Ontario, Canada. J. Geophys. Res. 104, 15975–15984.

Lenschow, D.H., Pearson, R., Stankov, B.B., 1982. Measurements of ozone vertical flux to ocean and forest. J. Geophys. Res. 87, 8833–8837.

Lenschow, D.H., Mann, J., Kristensen, L., 1994. How long is long enough when measuring fluxes and other turbulence statistics? J. Atmos. Ocean. Technol. 11, 661–673.

Leuning, R., King, K.M., 1992. Comparison of eddy-covariance measurements of $CO_2$ fluxes by open- and closed-path $CO_2$ analysers. Bound.-Lay. Meteorol. 59, 297–311.

Leuning, R., Moncrieff, J., 1990. Eddy-covariance $CO_2$ flux measurements using open- and closed-path $CO_2$ analysers: corrections for analyser water vapour sensitivity and damping of fluctuations in air sampling tubes. Bound.-Lay. Meteorol. 53, 63–76.

Lindroth, A., Grelle, A., Moren, A.S., 1998. Long-term measurements of boreal forest carbon balance reveal large temperature sensitivity. Glob. Change Biol. 4, 443–450.

Mahrt, L., 1982. Momentum balance of gravity flows. J. Atmos. Sci. 39, 2701–2711.

Mahrt, L., Vickers, D., Nakamura, R., Soler, M.R., Sun, J., Burns, S., Lenschow, D.H., 2001. Shallow drainage flows. Bound.-Lay. Meteorol. 101, 243–260.

Malhi, Y., Nobre, A.D., Grace, J., Kruijt, B., Pereira, M.G.P., Culf, A., Scott, S., 1998. Carbon dioxide transfer over a Central Amazonian rain forest. J. Geophys. Res. 103, 31593–31612.

Mann, J., Lenschow, D.H., 1994. Errors in airborne flux measurements. J. Geophys. Res. 99, 14519–14526.

Massman, W.J., 2000. A simple method for estimating frequency response corrections for eddy covariance systems. Agric. For. Meteorol. 104, 185–198.

Massman, W.J., 2001. Reply to comment by Rannik on "A simple method for estimating frequency response corrections for eddy covariance systems". Agric. For. Meteorol. 107, 247–251.

Massman, W.J., Sommerfeld, R.A., Mosier, R.A., Zeller, K.F., Hehn, T.J., Rochelle, S.G., 1997. A model investigation of turbulent-driven pressure-pumping effects on the rate of diffusion of $CO_2$, $N_2O$, and $CH_4$ through layered snowpacks. J. Geophys. Res. 102, 18851–18863.

McMillen, R.T., 1988. An eddy correlation technique with extended applicability to non-simple terrain. Bound.-Lay. Meteorol. 43, 231–245.

McNaughton, K.G., Laubach, J., 2000. Power spectra and cospectra for wind and scalars in a disturbed surface layer at the base of an advective inversion. Bound.-Lay. Meteorol. 96, 143–185.

Moncrieff, J.B., Mahli, Y., Leuning, R., 1996. The propagation of errors in long-term measurements of land-atmosphere fluxes of carbon and water. Glob. Change Biol. 2, 231–240.

Moore, C.J., 1986. Frequency response corrections for eddy correlation systems. Bound.-Lay. Meteorol. 37, 17–35.

Mulhearn, P.J., 1977. Relations between surface fluxes and mean profiles of velocity, temperature and concentration downwind of a change in surface roughness. Quart. J. R. Meteorol. Soc. 103, 785–802.

Munger, J.W., Wofsy, S.C., Bakwin, P.S., Fan, S.-M., Goulden, M.L., Daube, B.C., Goldstein, A.H., 1996. Atmospheric deposition of reactive nitrogen oxides and ozone in a temperate deciduous forest and a subarctic woodland: measurement and mechanisms. J. Geophys. Res. 101, 12639–12657.

Nilson, R.H., Peterson, E.W., Lie, K.H., 1991. Atmospheric pumping: a mechanism causing vertical transport of contaminated gases through fractured permeable media. J. Geophys. Res. 96, 21948–21993.

Paw U, K.T., Shaw, R.H., Maitani, T., Cionco, R.M., 1989. Gravity waves in an almond orchard. In: Proceedings of the 19th Conference on Agricultural and Forest Meteorology. American Meteorological Society, Boston, MA, pp. 184–185.

Paw U, K.T., Shaw, R.H., Maitani, T., 1990. Gravity waves, coherent structures, and plant canopies. In: Proceedings of the Ninth Symposium on Turbulence and Diffusion. American Meteorological Society, Boston, MA, pp. 244–246.

Paw U, K.T., Baldocchi, D.D., Meyers, T.P., Wilson, K.B., 2000. Correction of eddy-covariance measurements incorporating both advective effects and density fluxes. Bound.-Lay. Meteorol. 97, 487–511.

Philip, J.R., 1959. The local theory of advection. I. J. Meteorol. 16, 535–547.

Pilgaard, K., Hummelshøj, P., Jensen, N.O., Chen, Z., 2001. Two years of continuous $CO_2$ eddy-flux measurements over a Danish beech forest. Agric. For. Meteorol. 107, 29–41.

Rannik, Ü., 2001. A comment on the paper by W.J. Massman "A simple method for estimating frequency response corrections for eddy covariance systems". Agric. For. Meteorol. 107, 241–245.

Rannik, Ü., Vesala, T., Keskinen, R., 1997. On the damping of temperature fluctuations in a circular tube relevant to the eddy covariance measurement technique. J. Geophys. Res. 102, 12789–12794.

Raupach, M.R., Weng, W.S., Carruthers, D.J., Hunt, J.C.R., 1992. Temperature and humidity fields and fluxes over low hills. Quart. J. R. Meteorol. Soc. 118, 191–225.

Sakai, R.K., Fitzjarrald, D.R., Moore, K.E., 2001. Importance of low-frequency contributions to eddy fluxes observed over rough surfaces. J. Appl. Meteorol. 40, 2178–2192.

Schmid, H.P., 1994. Source areas for scalar and scalar fluxes. Bound.-Lay. Meteorol. 67, 293–318.

Schmid, H.P., Grimmond, C.S.B., Cropley, F., Offerle, B., Su, H.B., 2000. Measurements of $CO_2$ and energy fluxes over a mixed hardwood forest in the mid-western United States. Agric. For. Meteorol. 103, 357–374.

Shaw, R.H., Zhang, X.J., 1992. Evidence of pressure-forced turbulent flow in a forest. Bound.-Lay. Meteorol. 58, 273–288.

Shaw, W.J., Spicer, C.W., Kenny, D.V., 1998. Eddy correlation fluxes of trace gases using a tandem mass spectrometer. Atmos. Environ. 32, 2887–2898.

Smith, R.B., 1979. The influence of mountain on the atmosphere. Adv. Geophys. 21, 87–230.

Sun, J., Esbensen, S.K., Mahrt, L., 1995. Estimation of surface heat flux. J. the Atmos. Sci. 52, 3162–3171.

Sun, J., Desjardins, R., Mahrt, L., MacPherson, I., 1998. Transport of carbon dioxide, water vapor, and ozone by turbulence and local circulations. J. Geophys. Res. 103, 25873–25885.

Suyker, A.E., Verma, S.B., 1993. Eddy correlation measurement of $CO_2$ flux using a closed-path sensor: theory and field tests against an open path sensor. Bound.-Lay. Meteorol. 64, 391–407.

Tanner, C.B., Thurtell, G.W., 1969. Anemoclinometer measurements of Reynolds stress and heat transport in the atmospheric surface layer. Department of Soil Science, University of Wisconsin, Madison, WI, Research and Development Tech Report ECOM 66-G22-F to the US Army Electronics Command.

Tanner, B.D., Swiatek, E., Greene, J.P., 1993. Density fluctuations and use of the krypton hygrometer in surface flux measurements. In: Allen, R.G. (Ed.), Management of Irrigation and Drainage Systems. American Society of Civil Engineers, New York, NY, pp. 945–952.

Webb, E.K., Pearman, G.I., Leuning, R., 1980. Correction of flux measurements for density effects due to heat and water vapor transfer. Quart. J. R. Meteorol. Soc. 106, 85–106.

Weber, R.O., 1999. Remarks on the definition and estimation of friction velocity. Bound.-Lay. Meteorol. 93, 197–209.

Wilczak, J.M., Edson, J.B., Høgstrup, J., Hara, T., 1999. The budget of turbulent kinetic energy in the marine atmospheric

surface layer. In: Geernaert, G.L. (Ed.), Air–Sea Exchange: Physics, Chemistry, and Dynamics. Kluwer Academic Publishers, Dordrecht, The Netherlands, pp. 153–173.

Wilczak, J.M., Oncley, S.P., Stage, S.A., 2001. Sonic anemometer tilt correction algorithms. Bound.-Lay. Meteorol. 99, 127–150.

Wilson, J.D., Finnigan, J.J., Raupach, M.R., 1998. A first-order closure for disturbed plant-canopy flows and its application to winds in a canopy on a ridge. Quart. J. R. Meteorol. Soc. 124, 705–732.

Wofsy, S.C., Hollinger, D.Y., for the AmeriFlux science team 1998. Scientific Plan for AmeriFlux: US Long-Term Flux Measurement Network. http://cdiac.esd.ornl.gov/pro-grams/ameriflux/scif.htm.

Wofsy, S.C., Goulden, M.L., Munger, J.W., Fan, S.M., Bakwin, P.S., Daube, B.C., Bassow, S.L., Bazzaz, F.A., 1993. Net exchange of $CO_2$ in a midlatitude forest. Science 260, 1314–1317.

Wyngaard, J.C., Coté, O.R., 1972. Cospectral similarity in the atmospheric surface layer. Quart. J. R. Meteorol. Soc. 98, 590–603.

Wyngaard, J., Kosovic, B., 1994. Similarity of structure-function parameters in the stably stratified boundary-layer. Bound.-Lay. Meteorol. 71, 277–296.

Yang, P.C., 1998. Carbon dioxide flux within and above a boreal aspen forest. Ph.D. Thesis. University of British Columbia, Vancouver, Canada.